UNCLASSIFIED CONFIDENTIAL

C. 2 6

Copy
RM E54F07

NACA RM E54F07

NACA

RESEARCH MEMORANDUM

PERFORMANCE CHARACTERISTICS OF SEVERAL FULL-SCALE DOUBLE-SHROUD EJECTOR CONFIGURATIONS OVER A RANGE OF PRIMARY GAS TEMPERATURES

By William K. Greathouse

Lewis Flight Propulsion Laboratory
Cleveland, Ohio

LIBRARY COPY

AUG 19 1954

LANGLEY AERONAUTICAL LABORATORY
LIBRARY, NACA
LANGLEY FIELD, VIRGINIA

CLASSIFICATION CHANGED

UNCLASSIFIED

To _____

By authority of Nasa TPA 9 Date Effective 9-1-59

NB 11-20-59

CLASSIFIED DOCUMENT

This material contains information affecting the National Defense of the United States within the meaning of the espionage laws, Title 18, U.S.C., Secs. 793 and 794, the transmission or revelation of which in any manner to an unauthorized person is prohibited by law.

NATIONAL ADVISORY COMMITTEE FOR AERONAUTICS

WASHINGTON
August 19, 1954

CONFIDENTIAL

UNCLASSIFIED

NASA Technical Library
3 1176 01435 4139

NATIONAL ADVISORY COMMITTEE FOR AERONAUTICS

RESEARCH MEMORANDUM

PERFORMANCE CHARACTERISTICS OF SEVERAL FULL-SCALE DOUBLE-SHROUD EJECTOR CONFIGURATIONS OVER A RANGE OF PRIMARY GAS TEMPERATURES

By William K. Greathouse

3400
CM-1

SUMMARY

An experimental investigation was conducted on eight double-shroud ejector configurations which utilized a current production-type turbojet engine and an afterburner as the primary gas generator. The test configurations simulated the geometry of an afterburner installation that had a two-position variable-area nozzle which was actuated by linkage to a translating shroud. An inner and an outer passage were formed by the variable-area nozzle, the translating shroud, and the ejector shroud to make what is known in ejector literature as a double-shroud ejector.

Air-flow and thrust characteristics of each ejector configuration are presented for a range of operating pressure ratios and weight-flow ratios at representative nonafterburning or afterburning primary gas temperatures. The over-all performance of the double-shroud ejectors was similar to the pumping and thrust performance of single-shroud ejectors having about the same exit geometry. Ejector thrust attained at high cooling air flows indicated the recovery of about 96 percent of the thrust ideally available from an ejector system with complete isentropic expansion. There was some recirculatory flow of gas from the primary stream back through the tertiary passage at low values of cooling air flow.

INTRODUCTION

The air ejector has been established as a means of providing a suitable jet-exit configuration with respect to thrust performance and as a method of cooling aircraft power plant installations. Single-shroud ejectors are used primarily in connection with engine tail-pipe or afterburner cooling. A double-shroud ejector may be utilized when additional air flow is necessary for purposes such as air frame structural cooling.

UNCLASSIFIED

Pumping and gross thrust characteristics of numerous single-shroud small-scale ejectors are reported in references 1 to 9 for configurations having conical, cylindrical, and divergent shrouds. The performance of some full-scale conical and cylindrical single-shroud ejectors is given in references 10 and 11. Double-shroud ejector performance is presented in references 12 to 14 for a limited number of small-scale ejector configurations in which the air to each passage was independently supplied. References 12 and 13 are for the special case of secondary total pressure (inner cooling air passage) equal to tertiary total pressure (outer cooling air passage). The case in which the amount of air flow through each passage is maintained at various constant values is investigated in reference 14. Because information on the performance of full-scale double-shroud ejectors with a common air supply for the secondary and tertiary passages is nonexistent, a brief investigation of their over-all performance characteristics has been conducted at the NACA Lewis laboratory. 3400

The ejector-afterburner configurations described in this report simulated the geometry of an afterburner installation that utilized a translating shroud to actuate the variable-area afterburner nozzle, all of which were submerged in a cavity similar to the aft fuselage of an airplane. An inner passage between the afterburner nozzle and the translating shroud and an outer passage between the translating shroud and the ejector shroud formed the double-shroud ejector configurations. Over-all pumping and thrust characteristics of eight such configurations, mounted on a turbojet engine in an altitude test chamber, were measured and are reported herein.

APPARATUS AND INSTRUMENTATION

Test Facility

The double-shroud ejector tests of this investigation were performed on a current production-type turbojet engine and afterburner assembly arranged in an altitude chamber as schematically shown in figure 1. The engine-afterburner-ejector assembly was rigidly mounted to a platform that was suspended from the top of the altitude chamber by means of steel flexure plates. Scale thrust force transmitted from the platform to the null-type thrust measuring unit could be determined accurately to within ±1 percent.

Engine and ejector air were supplied from either the atmosphere or the laboratory air system and were separately controlled. A bulkhead, which incorporated a labyrinth seal around the forward end of the engine, provided for freedom of engine movement in the axial direction and permitted the simulation of flight conditions by independently varying inlet total pressure and exhaust static pressure.

Test Configurations

The typical test configuration in figure 1 consisted of an afterburner (fig. 2) submerged within a cooling shroud (fig. 3) which carried an inner shroud (fig. 4) so as to form an inner (secondary) passage and an outer (tertiary) passage as shown in figures 5 and 6 for typical ejectors. Figure 5 indicates the flow passage geometry that resulted with the nonafterburning primary nozzle and the inner shroud in a retracted position; figure 6 indicates the geometry with the afterburning primary nozzle and the inner shroud in the extended position.

3400

CM-1 back

Five different ejector shrouds were installed on the cooling shroud to provide the eight ejector configurations shown in figure 7 and listed in the following table:

Ejector configuration	Primary nozzle exit diameter, in.	Inner shroud position	Diameter ratio	Spacing ratio	Ejector shroud used
1	19.27	Retracted	1.41	0.93	1
3[a]	↓	↓	1.50	.47	3
4	↓	↓	1.55	.36	4
5	↓	↓	1.45	.18	None
6	↓	↓	1.45	(b)	6
1 AB	24.93	Extended	1.10	.69	1
3 AB	↓	↓	1.16	.36	3 and part of 6
4 AB	↓	↓	1.27	.25	4

[a]The investigation of configuration 2 was discontinued because of time limitation.

[b]Spacing ratio not defined because of faired ejector exit.

A photograph of shroud 1 is shown in figure 8 and is typical of shrouds 3 and 4. The shape of shroud 6 is indicated by the assembly photograph of ejector configuration 6 in figure 9, which represents an ejector-fuselage exit combination having a large blunt base area. The lower section of shroud 6 and all of shroud 3 were combined to form configuration 3AB.

Instrumentation

The axial locations of various ejector instrumentation stations are given in figures 3, 5, and 6.

Pressure instrumentation. - Primary total pressure P_p was measured at station p with a water-cooled rake consisting of 13 probes spaced on equal flow areas across the afterburner diameter. Secondary total pressure P_s was measured at station s with one three-probe rake and seven single probes equally spaced around the secondary passage circumference. Tertiary total pressure P_t was measured with eight single probes at station t equally spaced around the tertiary passage circumference. Plenum chamber total pressure P_B was measured at station b by six pressure taps spaced along the plenum chamber wall. Ambient exhaust pressure P_0 was measured with four equally spaced probes located on the outside of the ejector shroud near the exit. The primary static pressure p_p was measured at station p by eight equally spaced wall taps on the afterburner shell. 3400

Temperature instrumentation. - Primary (turbine discharge) total temperature T_p for nonafterburning operation was measured with eight thermocouple probes between the turbine discharge and the afterburner fuel spray bars. The accuracy of turbine discharge temperature measurement was believed to be well within $\pm 20^{\circ}$ R. For afterburning operation the primary total temperature was calculated (see appendix B) from the flow conditions determined at station p. Secondary total temperature T_s was measured by four equally spaced thermocouple probes at station s, while tertiary total temperature T_t was measured by four equally spaced thermocouple probes at station t. Cooling air temperature T_c was measured by a single thermocouple in the cooling air line upstream of the plenum chamber.

Flow determination. - Primary gas flow W_p was computed as the sum of engine inlet air and total fuel minus leakage air in the conventional manner. Cooling air flow W_c was measured with an A.S.M.E. standard flat-plate orifice and also computed from total- and static-pressure measurements taken in the cooling air pipe. Tertiary air flow W_t was computed from measurements taken with four pitot tubes (figs. 5 and 6) equally spaced around the tertiary flow passage, while secondary air flow W_s was taken as the difference between cooling air flow and tertiary air flow.

The measurement of ejector jet thrust was obtained from the scale thrust reading after accounting for the forces acting on the test rig due to the cooling air supply system and the engine labyrinth seal. Symbols and the method of calculating various ejector parameters are further defined in appendixes A and B, respectively.

PROCEDURE

Each ejector configuration was investigated over a range of cooling air to primary gas weight-flow ratio W_c/W_p and a range of primary total to ambient exhaust pressure ratio P_p/p_0 at one or more representative primary gas temperatures. The range of conditions is presented in the following table:

[redacted]

Configuration	Afterburner	Primary gas temperature, T_p, °R	Primary pressure ratio, P_p/p_0	Weight-flow ratio, W_c/W_p
1	Nonafterburning	1550 to 1580	1.7 to 8.1	0 to 0.24
3	↓	1580 to 1610	1.6 to 7.0	0 to 0.22
4	↓	1570 to 1600	1.7 to 7.25	0 to 0.20
5	↓	1540 to 1580	2.0 to 7.75	0 to 0.20
6	↓	1550 to 1600	1.7 to 5.25	0 to 0.20
1 AB	Afterburning	2050 to 2200	1.5 to 7.85	0 to 0.12
1 AB	↓	2700 to 2800	1.6 to 5.8	0 to 0.12
3 AB	↓	2250 to 2300	1.5 to 5.5	0
3 AB	↓	2720 to 2820	1.75 to 5.9	0.02 to 0.12
4 AB	↓	2050 to 2100	1.75 to 7.2	0
4 AB	↓	2670 to 2760	1.75 to 6.0	0.02 to 0.12

RESULTS AND DISCUSSION

Pumping Characteristics

The pumping performance of each ejector configuration is presented in figures 10 through 18 for the specific primary gas temperature at which the test was performed. The typical manner in which the test data were first plotted as obtained at constant values of primary pressure ratio is represented in figure 10 only for configuration 1. Pumping performance of the other configurations (including 1) is presented conventionally in figures 11 through 18, as cross plots of curves such as figure 10, along with test data obtained at zero cooling air flow ($W_c/W_p = 0$).

These double-shroud ejector air-flow curves, based on plenum chamber pressure, exhibit characteristics very similar to those of single-shroud ejectors having about the same over-all exit diameter and spacing ratio. The usual ejector pumping action occurred (in the range of primary pressure ratios investigated) only for configurations 1, 3, 1AB, 3AB, and 4AB. Configurations 4, 5, and 6 showed little or no pumping ability because of the low spacing ratios involved. Ejectors of such low spacing ratio will handle cooling air flows in flight where ram pressure is available, but could serve for only minor cooling purposes at take-off. Pumping characteristics of configuration 1AB at a primary gas temperature of 2050° to 2200° R (fig. 16(a)) were practically the same as for a primary gas temperature of 2700° to 2800° R (fig. 16(b)).

Thrust Characteristics

Ejector thrust is presented in a manner similar to the pumping characteristics. Thrust data as obtained from the tests of configuration 1 are presented in figure 19. The cross-plotted figures 20

through 27 present ejector-thrust ratio F_{ej}/F_j of all the configurations over a range of primary pressure ratio for constant values of ejector weight-flow ratio. Ejector-thrust ratio F_{ej}/F_j is defined herein as the ratio of measured jet thrust of the ejector system to the jet thrust of a convergent nozzle operating at the same primary mass flow and primary pressure ratio as the ejector system and having an effective velocity coefficient $C_{v,e}$ of 0.98 (method of calculation is in appendix B).

The ejector thrust ratio curves for configurations 1, 3, 1AB, and 3AB show typical ejector thrust losses at or near zero cooling air flow (a pronounced dip in the $W_c/W_p = 0$ thrust ratio curve) when overexpansion and shock losses occurred in the primary stream at the particular operating primary pressure ratios (refs. 8 and 11). However, a considerable thrust increase was found for these configurations at other operating primary pressure ratios and more realistic cooling air flows. The remaining configurations (4, 5, 6, and 4AB) exhibited small thrust losses at low cooling air flows but showed only a slight increase in thrust with increased cooling air flow or operating pressure ratio. 3400

Isentropic ejector-thrust ratio $\frac{F_{ej}}{F_p' + F_c'}$, presented in figure 28 for configuration 1 only, indicates the actual ejector jet thrust attained in relation to the ideal thrust that would be available if the flows were expanded isentropically to ambient exhaust pressure. At the highest weight-flow ratio investigated ($W_c/W_p = 0.24$), a thrust of the order of 96 percent of the ideal thrust was attained by configuration 1 over the entire range of primary pressure ratio. Values of isentropic thrust ratio greater than 96 percent are indicated for weight-flow ratios exceeding 0.24. Inasmuch as a peak thrust ratio was not obtained with respect to pressure ratio or weight-flow ratio, it is apparent that this configuration operated overexpanded at all conditions investigated. The method of computing isentropic ejector-thrust ratio is defined in appendix B.

Secondary and Tertiary Systems

Total pressures and temperatures of the flow in the secondary and tertiary passages are presented for only the three ejector configurations (1AB, 3AB, and 4AB) that were operated at afterburning gas temperatures. Figures 29 to 31 give the ratio of average exit pressure $\frac{1}{2}(P_t + P_s)$ to plenum chamber pressure P_B, and figures 32 to 34 give the average temperature-rise ratio $\frac{\frac{1}{2}(T_s + T_t) - T_c}{T_c}$ for a range of ejector weight-flow ratio.

The ratio of tertiary to total cooling air flow is plotted in figure 35 for configuration 1AB. The considerable scatter of data resulted from computing tertiary air flow W_t from pitot-tube pressure measurements taken at the relatively low Mach number existing in the tertiary passage. Figure 36 shows the ratio of tertiary to secondary temperature T_t/T_s and the ratio of secondary to primary temperature T_s/T_p plotted against their respective weight-flow ratios, W_t/W_s and W_s/W_p. These data for configuration 1AB should be indicative of the tertiary and secondary flow conditions for configurations 3AB and 4AB for W_c/W_p values of the order of 0.06 to 0.12.

3400

It can be noted from figure 36 that the tertiary flow was sometimes greater and sometimes less than the secondary flow (W_t/W_s greater than 1.0 and less than 1.0). Also, at the lower values of W_t/W_s, the temperature of the tertiary exceeded the temperature of the secondary (T_t/T_s greater than 1.0) because the secondary pumping ability was somewhat greater than the tertiary pumping ability. Consequently, some of the hot primary stream gases near the ejector shroud wall (of relatively low velocity) were pulled back into the tertiary passage at several points by the excessive secondary suction or pumping action.

CONCLUDING REMARKS

The full-scale double-shroud ejector performance data presented herein provide additional information for the design of aircraft ejector installations. The pumping characteristics are, in general, similar to those of single-shroud ejectors. However, there appeared to be some recirculatory flow of gas from the primary stream back through the testing passage at low values of cooling air flow. The thrust attained by one double-shroud ejector at high cooling air flows indicated the recovery of 96 percent of the thrust ideally available from an ejector system with complete isentropic expansion.

Lewis Flight Propulsion Laboratory
National Advisory Committee for Aeronautics
Cleveland, Ohio, June 18, 1954

APPENDIX A

SYMBOLS AND PARAMETERS

The following symbols and parameters are used in this report:

A cross-sectional area of afterburner at station p, sq ft

$C_{v,e}$ effective velocity coefficient, ratio of measured jet thrust to jet thrust computed from measured mass flow and ideal effective velocity 3400

D_p exit diameter of primary nozzle, in.

D_s exit diameter of inner shroud, in.

D_t exit diameter of ejector shroud, in.

F_{ej} measured jet thrust of ejector system, lb

F_j calculated jet thrust of conical nozzle, lb

F_c' jet thrust of cooling air stream if measured mass flow were completely expanded isentropically, lb

F_p' jet thrust of primary stream if measured mass flow were completely expanded isentropically, lb

g acceleration due to gravity, 32.17 ft/sec^2

L_s axial distance from primary nozzle exit to inner shroud exit, in.

L_t axial distance from primary nozzle exit to ejector shroud exit, in.

P_B total pressure of cooling air in plenum chamber, lb/sq ft

P_p primary stream total pressure at station p, lb/sq ft

P_s secondary stream total pressure at station s, lb/sq ft

P_t tertiary stream total pressure at station t, lb/sq ft

p_p primary static pressure at station p, lb/sq ft

p_0 ambient or exhaust pressure, lb/sq ft

R gas constant for primary stream, approximately 53.3 (ft-lb)/(lb)($^{\circ}$R)

T_c measured cooling air temperature entering plenum chamber, °R

T_p measured or calculated primary stream total temperature, °R

T_s measured secondary total temperature at station s, °R

T_t measured tertiary total temperature at station t, °R

W_c cooling air entering plenum chamber, lb/sec

W_p primary stream gas flow, lb/sec

W_s secondary stream air flow, lb/sec

W_t tertiary stream air flow, lb/sec

γ ratio of specific heats of primary stream

3400

CM-2

APPENDIX B

METHODS OF CALCULATION

Ejector thrust ratio $\frac{F_{ej}}{F_j}$:

$$\frac{F_{ej}}{F_j} = \frac{F_{ej}}{C_{v,e}\left(\frac{W_p}{g}\right)V_{i,e}} = \frac{F_{ej}}{0.98 \times \left(\frac{W_p}{g}\right)V_{i,e}}$$

3400

Isentropic ejector-thrust ratio $\frac{F_{ej}}{F_p' + F_c'}$:

$$\frac{F_{ej}}{F_p' + F_c'} = \frac{F_{ej}}{\left(\frac{W_p}{g}\right)(V_{i,p}) + \left(\frac{W_c}{g}\right)(V_{i,c})} = \frac{F_{ej}}{\left(\frac{W_p}{g}\right)(V_{i,p})\left(1 + \frac{W_c}{W_p} \times \frac{V_{i,c}}{V_{i,p}}\right)}$$

Afterburning primary gas temperature T_p:

$$T_p = \frac{\left[\frac{p_p A}{W_p}\right]^2}{\left[\frac{pA}{W\sqrt{\frac{R}{g}T}}\right]_p^2 \left(\frac{R_p}{g}\right)}, \ ^\circ R$$

where

$V_{i,e}$ effective isentropic velocity (convergent nozzle velocity), computed by methods of reference 15 at existing P_p/p_0 and specific heat ratio of primary stream

$V_{i,p}$ isentropic velocity of complete expansion, computed by methods of reference 15 at existing P_p/p_0 and specific heat ratio of primary stream

$V_{i,c}$ isentropic velocity of complete expansion, computed by methods of reference 15 at specific heat ratio of 1.40 for existing P_B/p_0 of cooling air system. Assumed equal to zero when P_B/p_0 was less than 1.0

$\left[\frac{pA}{W\sqrt{\frac{R}{g}T}}\right]_p$ static pressure parameter for primary stream at station p. Computed from reference 15 at existing P_p/p_p and specific heat ratio

The quantities A, $C_{v,e}$, F_{ej}, F_j, F_p', F_c', g, P_B, P_p, p_p, p_0, R_p, W_c, and W_p are defined in appendix A. Specific heat ratio of the primary stream was determined from reference 16 at the known fuel-air ratio and the existing (or computed) primary gas temperature.

REFERENCES

1. Huddleston, S. C., Wilsted, H. D., and Ellis, C. W.: Performance of Several Air Ejectors with Conical Mixing Sections and Small Secondary Flow Rates. NACA RM E8D23, 1948.

2. Wilsted, H. D., Huddleston, S. C., and Ellis, C. W.: Effect of Temperature on Performance of Several Ejector Configurations. NACA RM E9E16, 1949.

3. Ellis, C. W., Hollister, D. P., and Sargent, A. F., Jr.: Preliminary Investigation of Cooling-Air Ejector Performance at Pressure Ratios from 1 to 10. NACA RM E51H21, 1951.

4. Kochendorfer, Fred D., and Rousso, Morris D.: Performance Characteristics of Aircraft Cooling Ejectors Having Short Cylindrical Shrouds. NACA RM E51E01, 1951.

5. Kochendorfer, Fred D.: Effect of Properties of Primary Fluid on Performance of Cylindrical Shroud Ejectors. NACA RM E53L24a, 1954.

6. Greathouse, W. K., and Hollister, D. P.: Preliminary Air-Flow and Thrust Calibrations of Several Conical Cooling-Air Ejectors with a Primary to Secondary Temperature Ratio of 1.0. I - Diameter Ratios of 1.21 and 1.10. NACA RM E52E21, 1952.

7. Greathouse, W. K., and Hollister, D. P.: Preliminary Air-Flow and Thrust Calibrations of Several Conical Cooling-Air Ejectors with a Primary to Secondary Temperature Ratio of 1.0. II - Diameter Ratios of 1.06 and 1.40. NACA RM E52F26, 1952.

8. Greathouse, W. K., and Hollister, D. P.: Air-Flow and Thrust Characteristics of Several Cylindrical Cooling-Air Ejectors with a Primary to Secondary Temperature Ratio of 1.0. NACA RM E52L24, 1953.

9. Huntley, S. C., and Yanowitz, Herbert: Pumping and Thrust Characteristics of Several Divergent Cooling-Air Ejectors and Comparison of Performance with Conical and Cylindrical Ejectors. NACA RM E53J13, 1954.

10. Wallner, Lewis E., and Jansen, Emmert T.: Full-Scale Investigation of Cooling Shroud and Ejector Nozzle for a Turbojet Engine - Afterburner Installation. NACA RM E51J04, 1951.

3400

CM- 2 back

11. Greathouse, W. K.: Preliminary Investigation of Pumping and Thrust Characteristics of Full-Size Cooling-Air Ejectors at Several Exhaust-Gas Temperatures. NACA RM E54A18, 1954.

12. Ellis, C. W., Hollister, D. P., and Wilsted, H. D.: Investigation of Performance of Several Double-Shroud Ejectors and Effect of Variable-Area Exhaust Nozzle on Single Ejector Performance. NACA RM E52D25, 1952.

13. Hollister, Donald P., and Greathouse, William K.: Performance of Double-Shroud Ejector Configuration with Primary Pressure Ratios from 1.0 to 10. NACA RM E52K17, 1953.

14. Reshotko, Eli: Performance Characteristics of a Double-Cylindrical-Shroud Ejector Nozzle. NACA RM E53H28, 1953.

15. Turner, L. Richard, Addie, Albert N., and Zimmerman, Richard H.: Charts for the Analysis of One-Dimensional Steady Compressible Flow. NACA TN 1419, 1948.

16. Pinkel, Benjamin, and Turner, L. Richard: Thermodynamic Data for the Computation of the Performance of Exhaust-Gas Turbines. NACA WR E-23, 1944. (Supersedes NACA ARR 4B25.)

3400

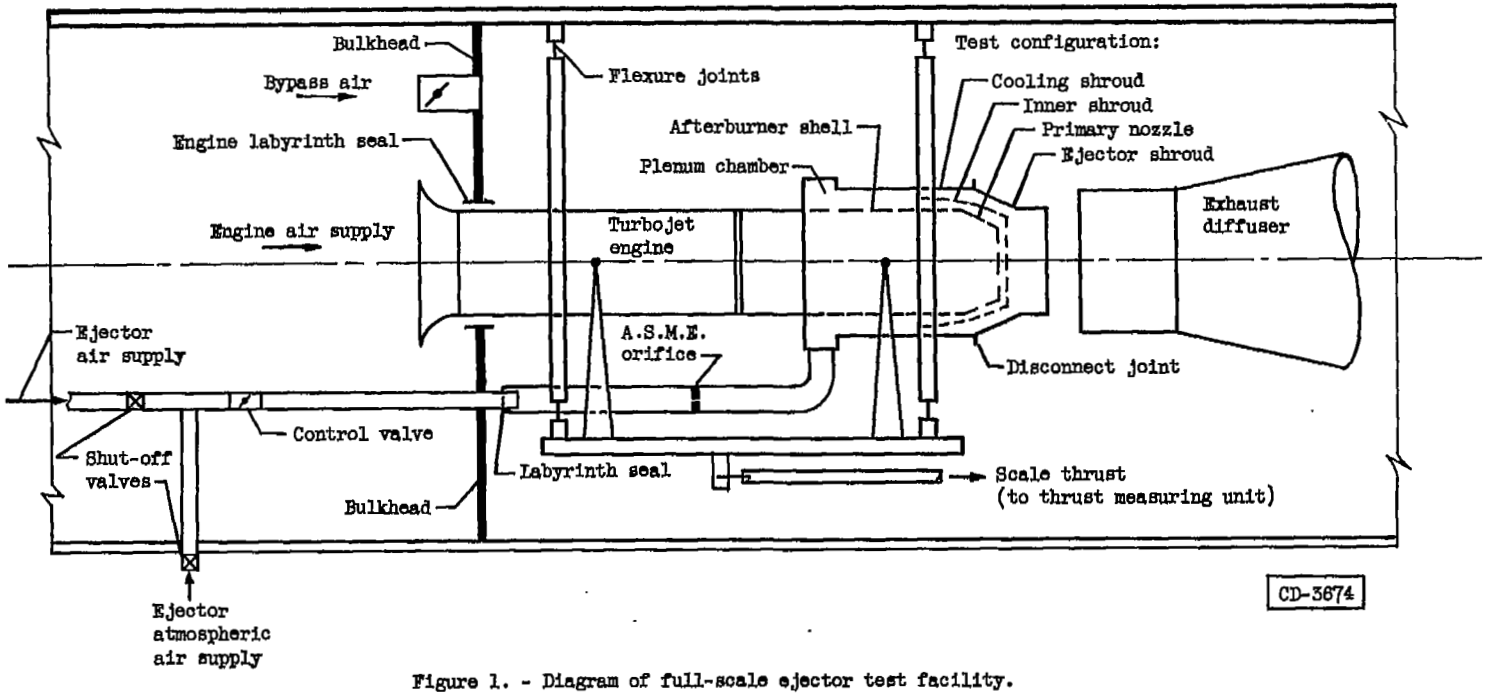

Figure 1. - Diagram of full-scale ejector test facility.

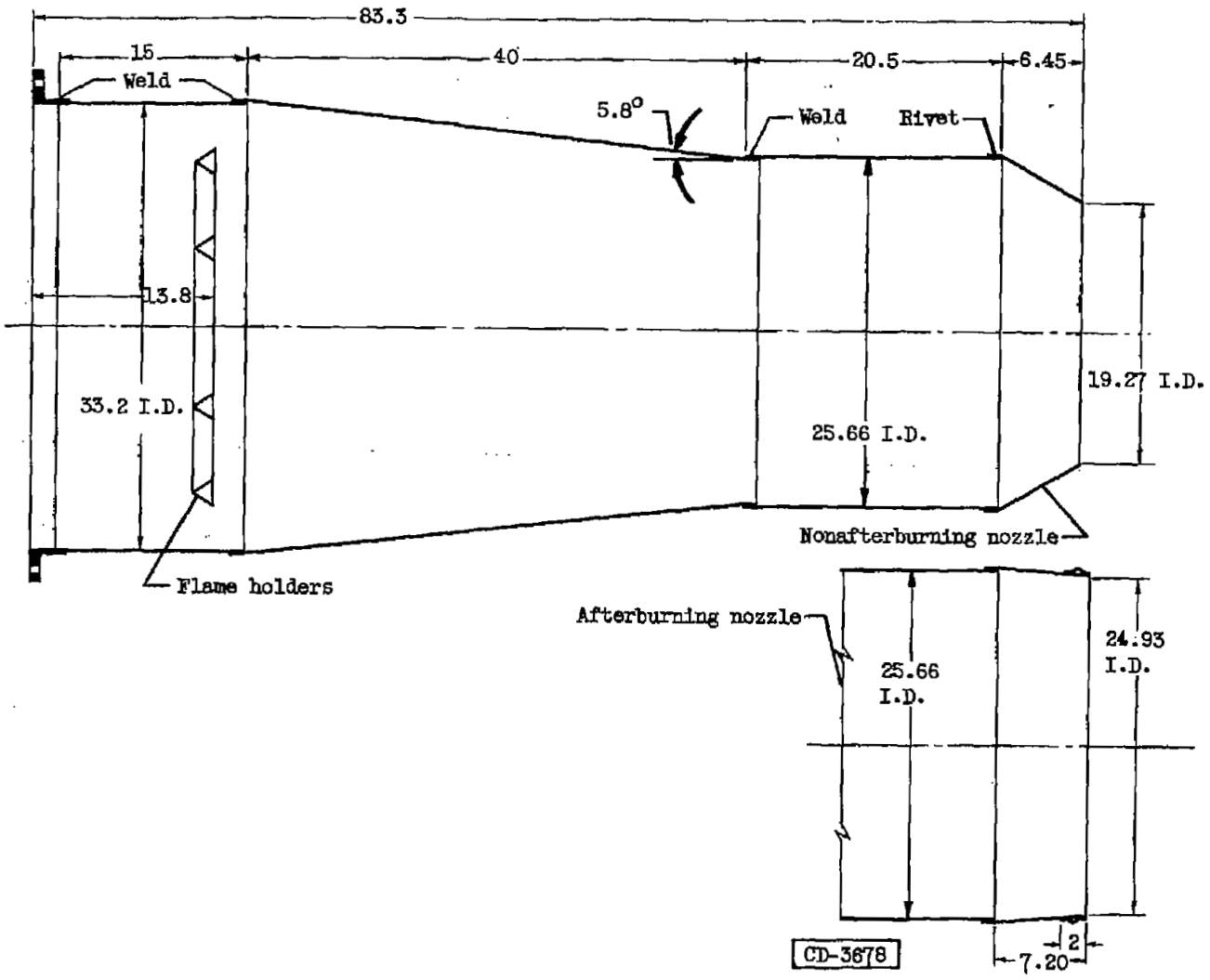

Figure 2. - Afterburner and primary nozzles. 19-9DL steel, 0.095 inch. (Dimensions are in inches unless otherwise indicated.)

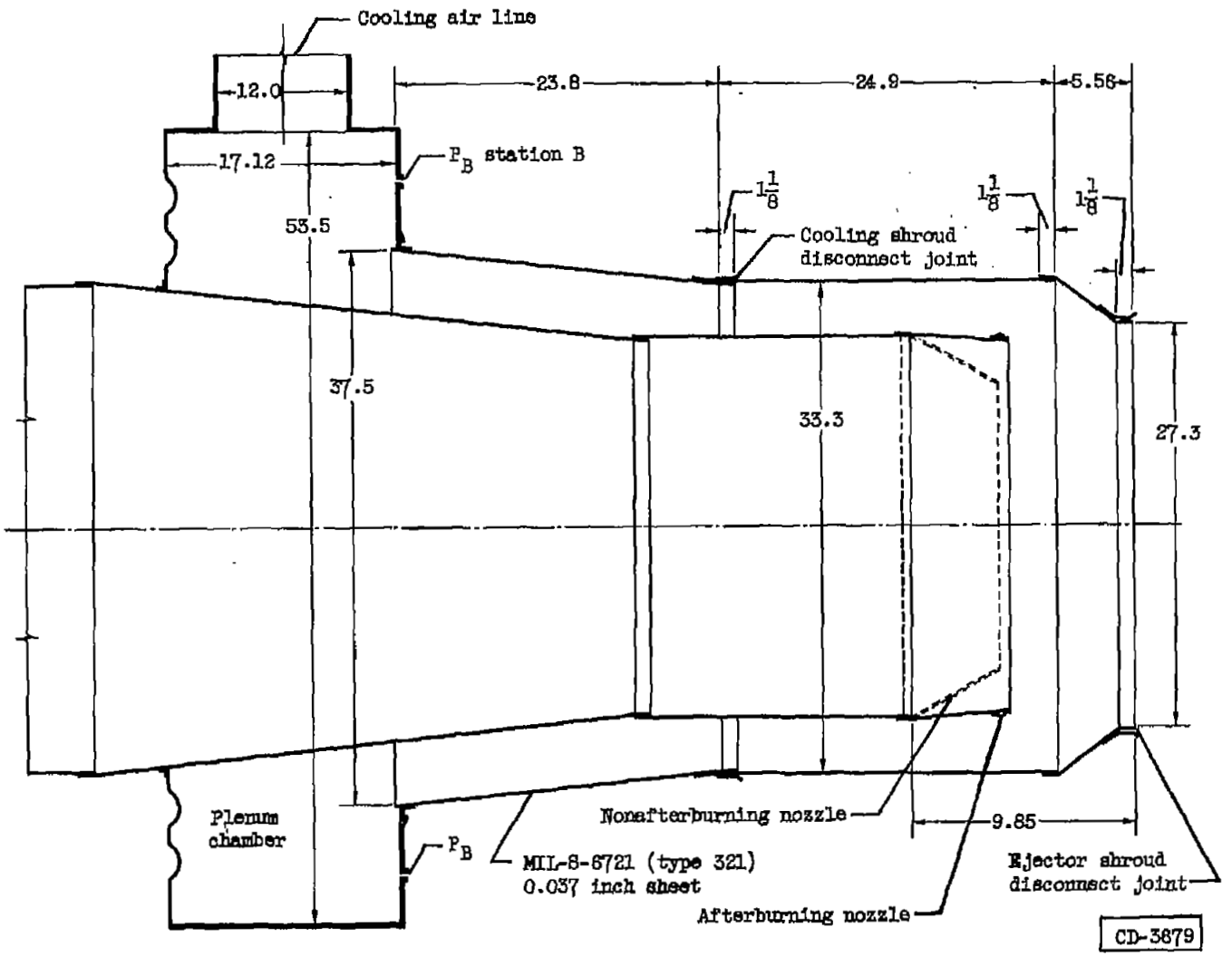

Figure 3. - Cooling shroud, plenum chamber, and afterburner assembly. (Dimensions are in inches.)

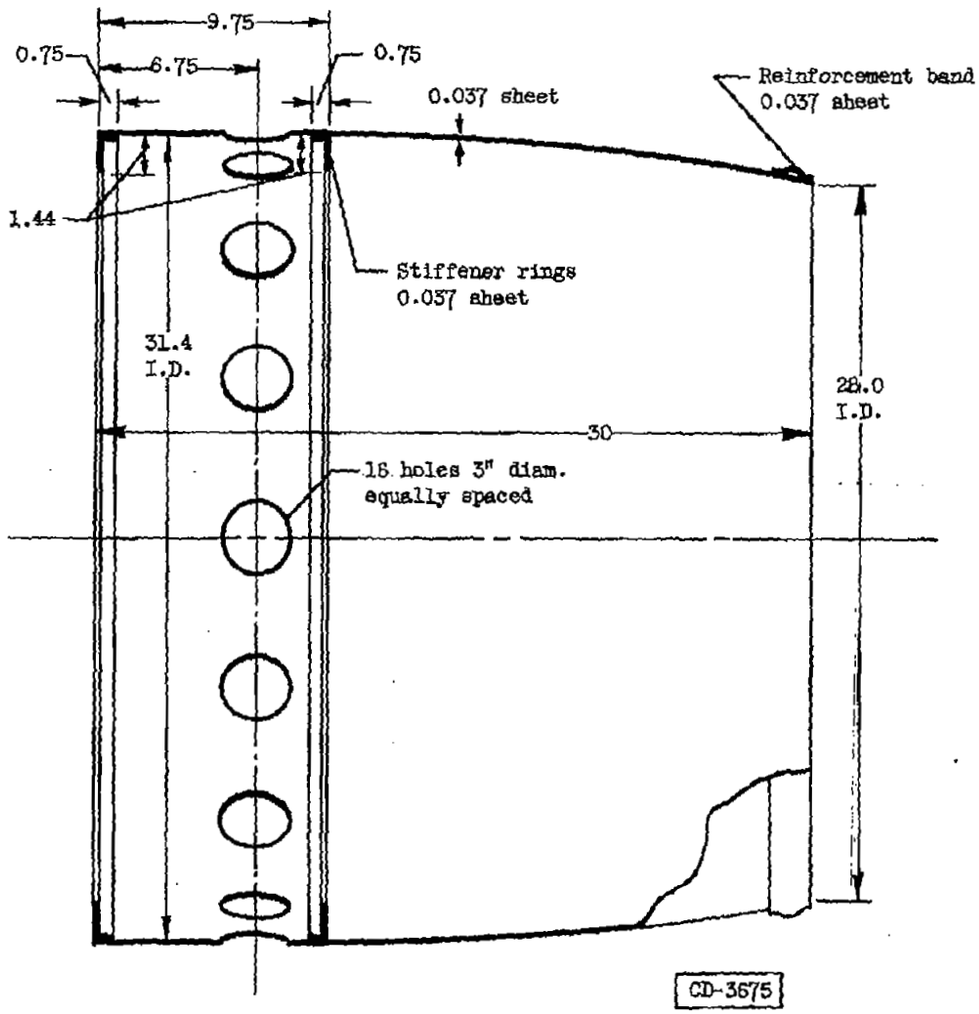

Figure 4. - Inner shroud. MIL-S-6721 (type 321) steel, 0.037 inch sheet. (Dimensions are in inches.)

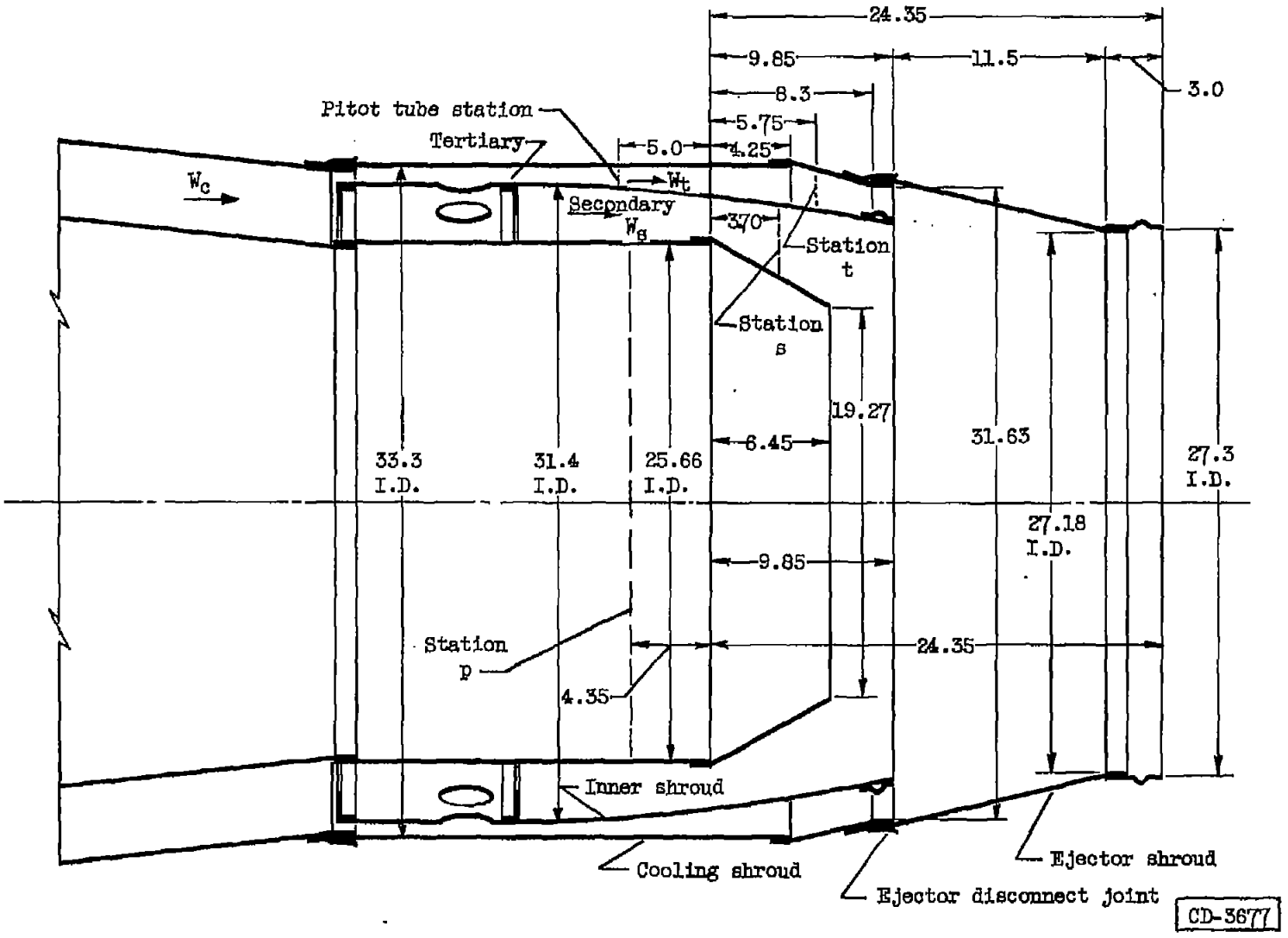

Figure 5. - Ejector configuration 1 (nonafterburning). (Dimensions are in inches.)

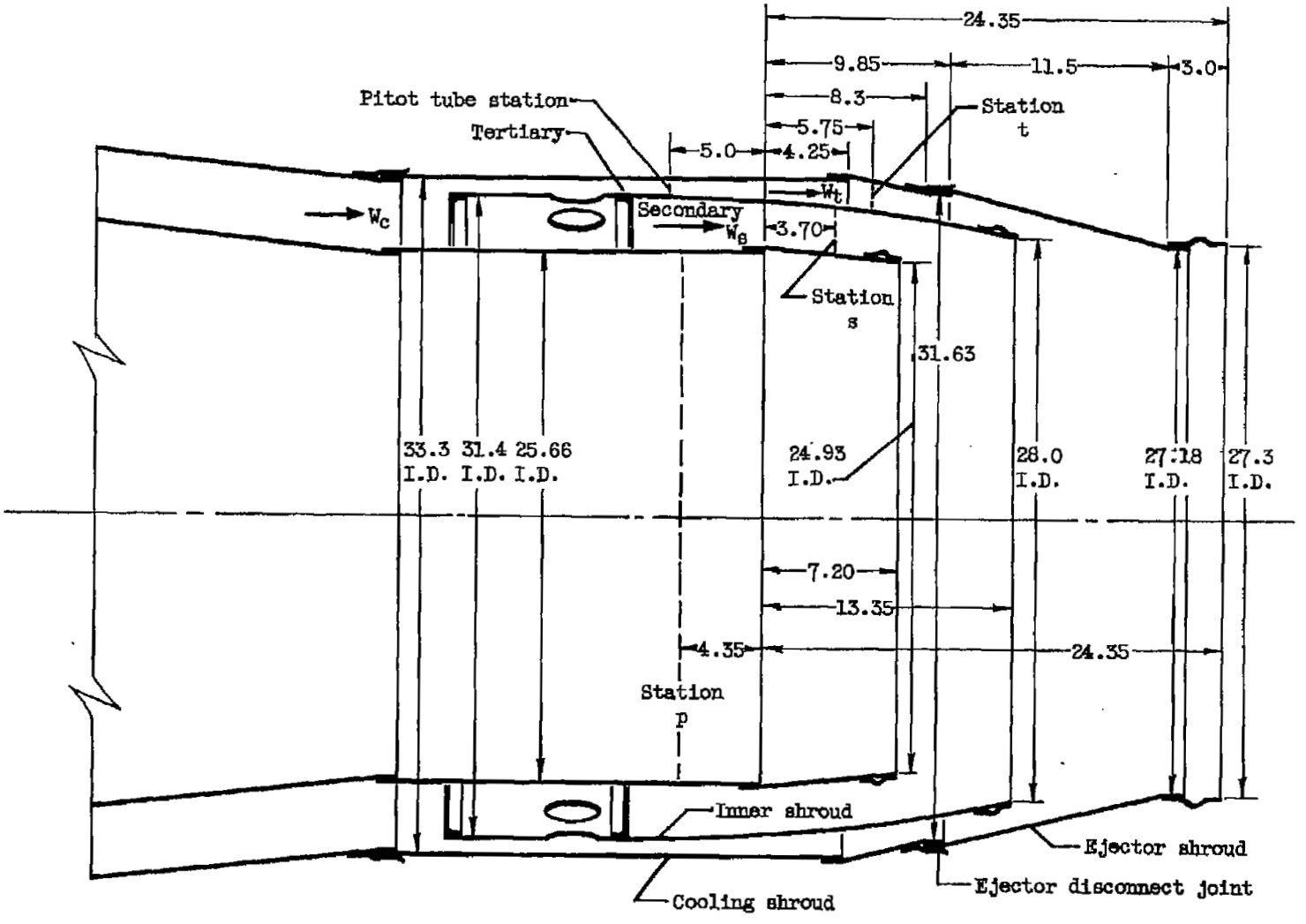

Figure 6. - Ejector configuration 1 AB (afterburning).

(Dimensions are in inches.)

CD-3676

CM-3 back 3400

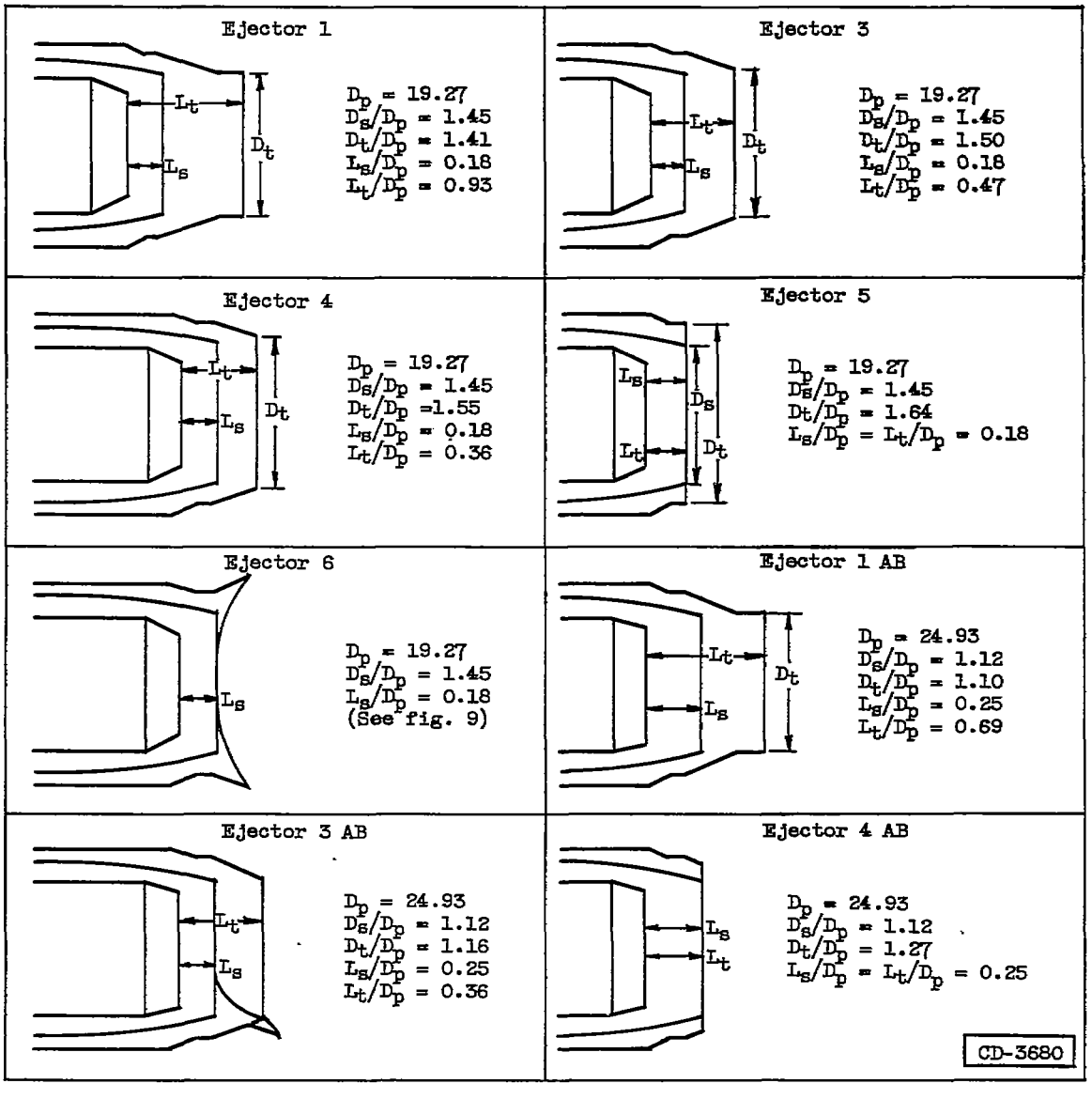

Figure 7. - Ejector configurations tested. D_p, primary nozzle exit diameter; D_s, inner shroud exit diameter. (All dimensions are inches at room temperature.)

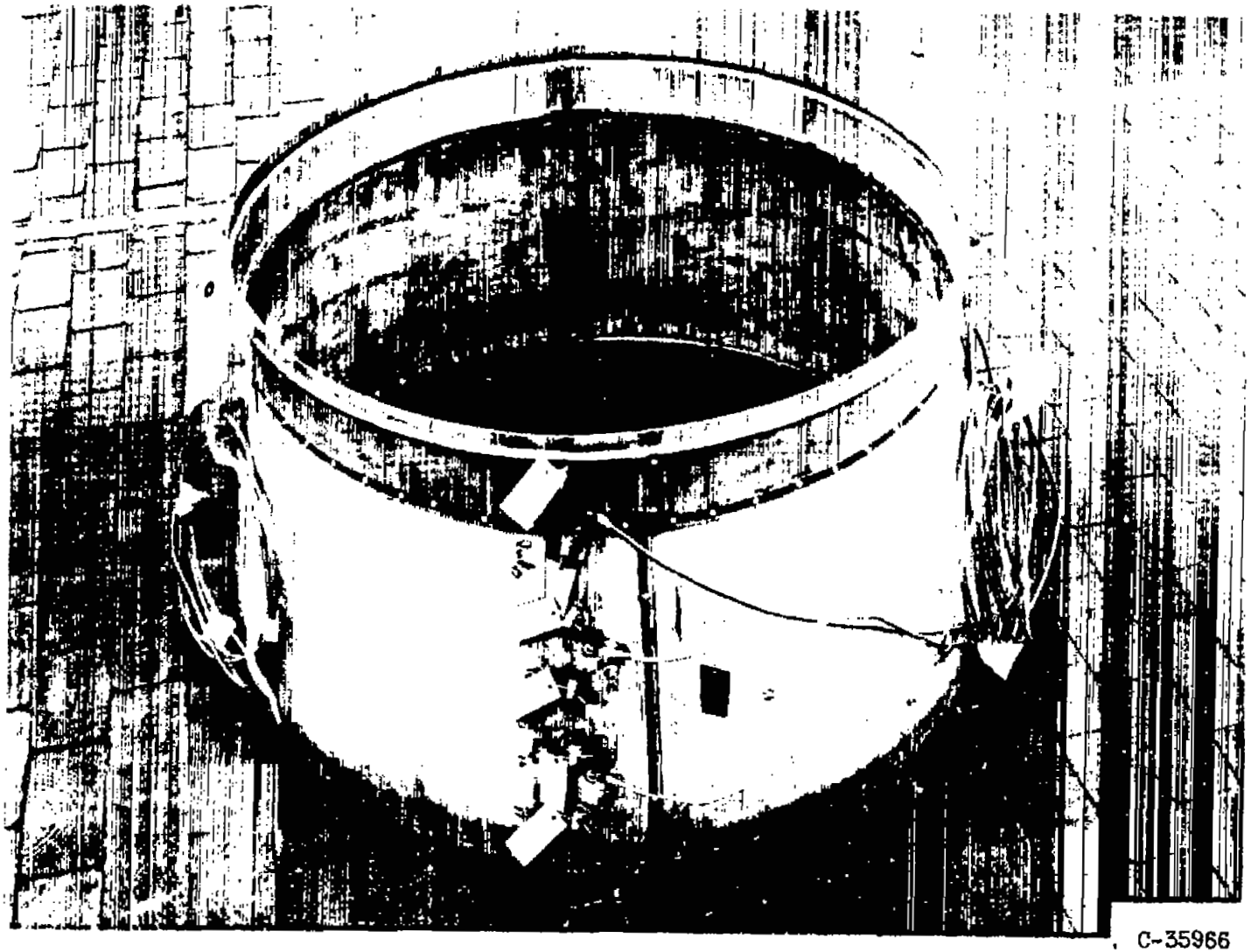

C-35966

Figure 8. - Ejector shroud for configurations 1 and 1 AB.

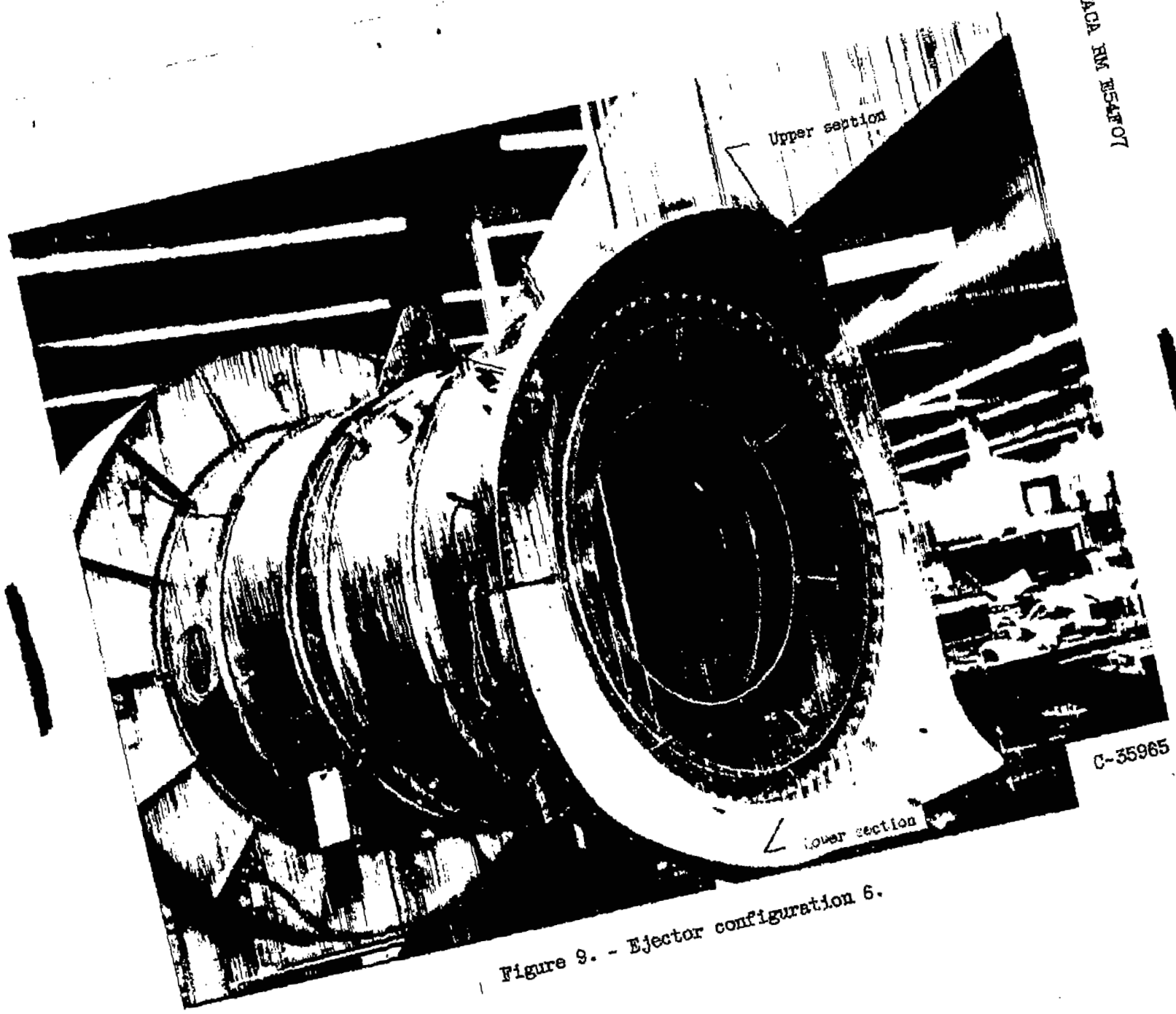

Figure 9. - Ejector configuration 6.

3400

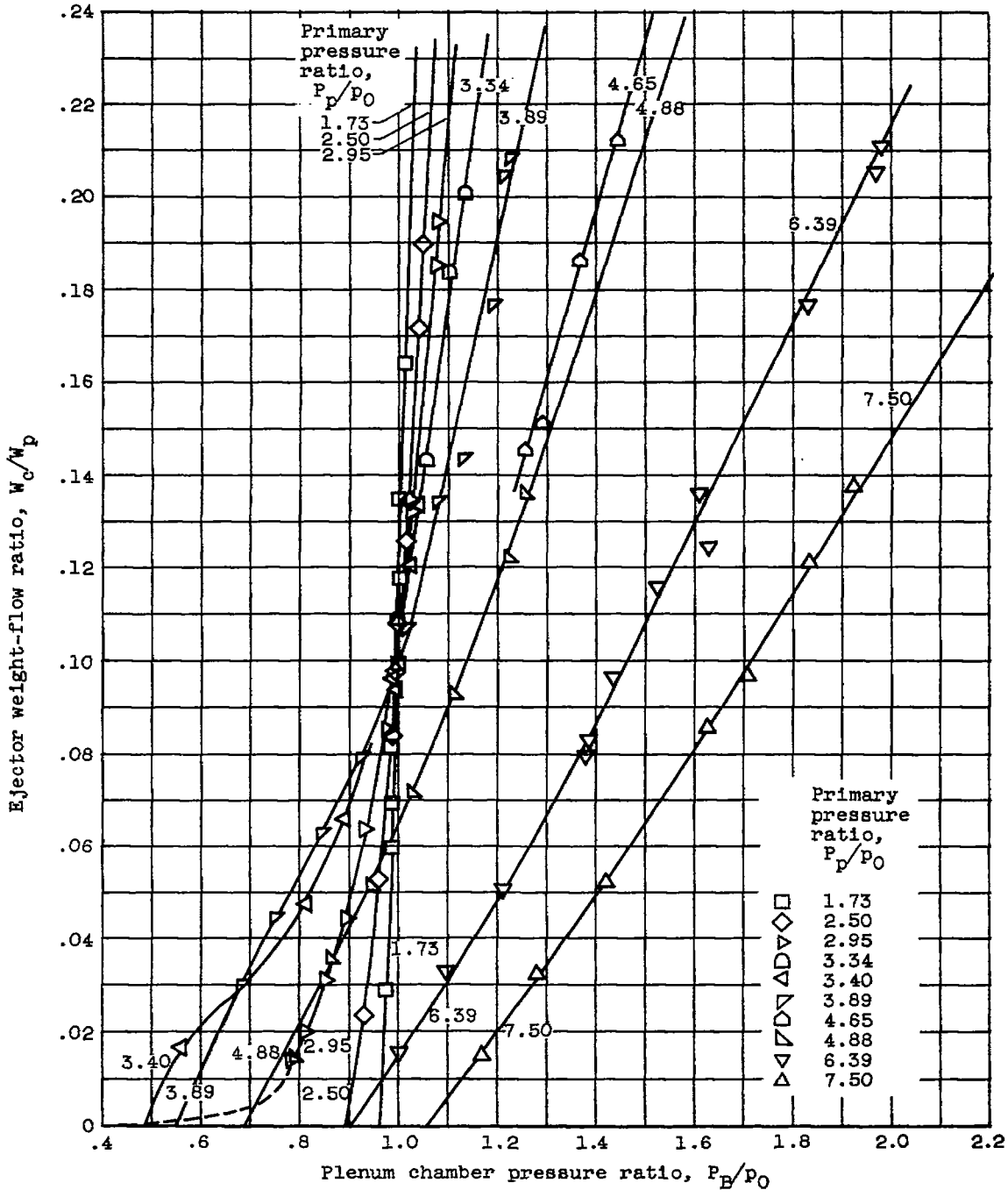

Figure 10. - Air flow data plot of ejector configuration 1. Primary gas temperatures from 1550° to 1580° R and cooling air supply temperature of 525° R.

3400

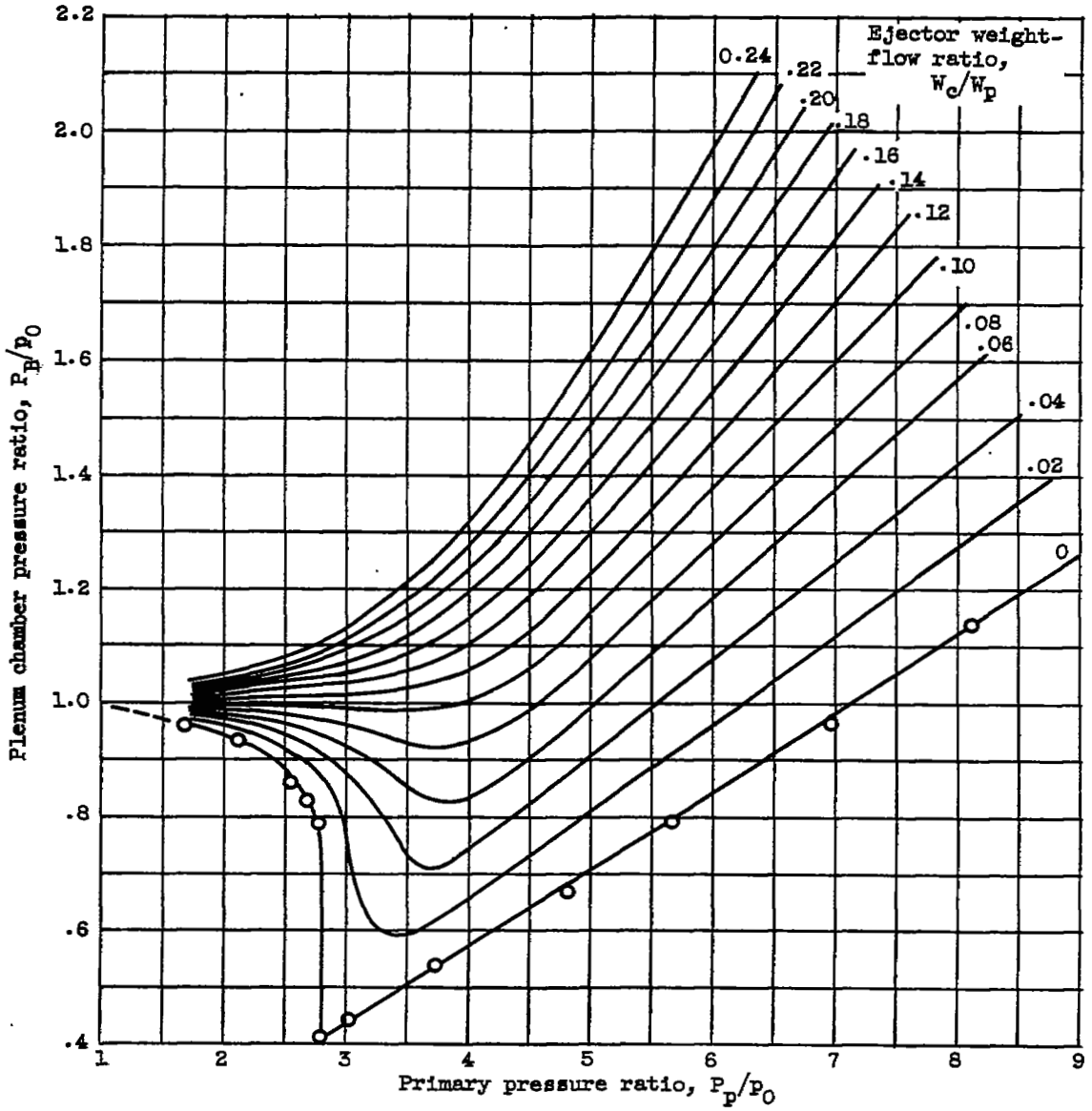

Figure 11. - Pumping characteristics of ejector configuration 1. Primary gas temperatures from 1550° to 1580° R and cooling air supply temperature of 525° R.

3400

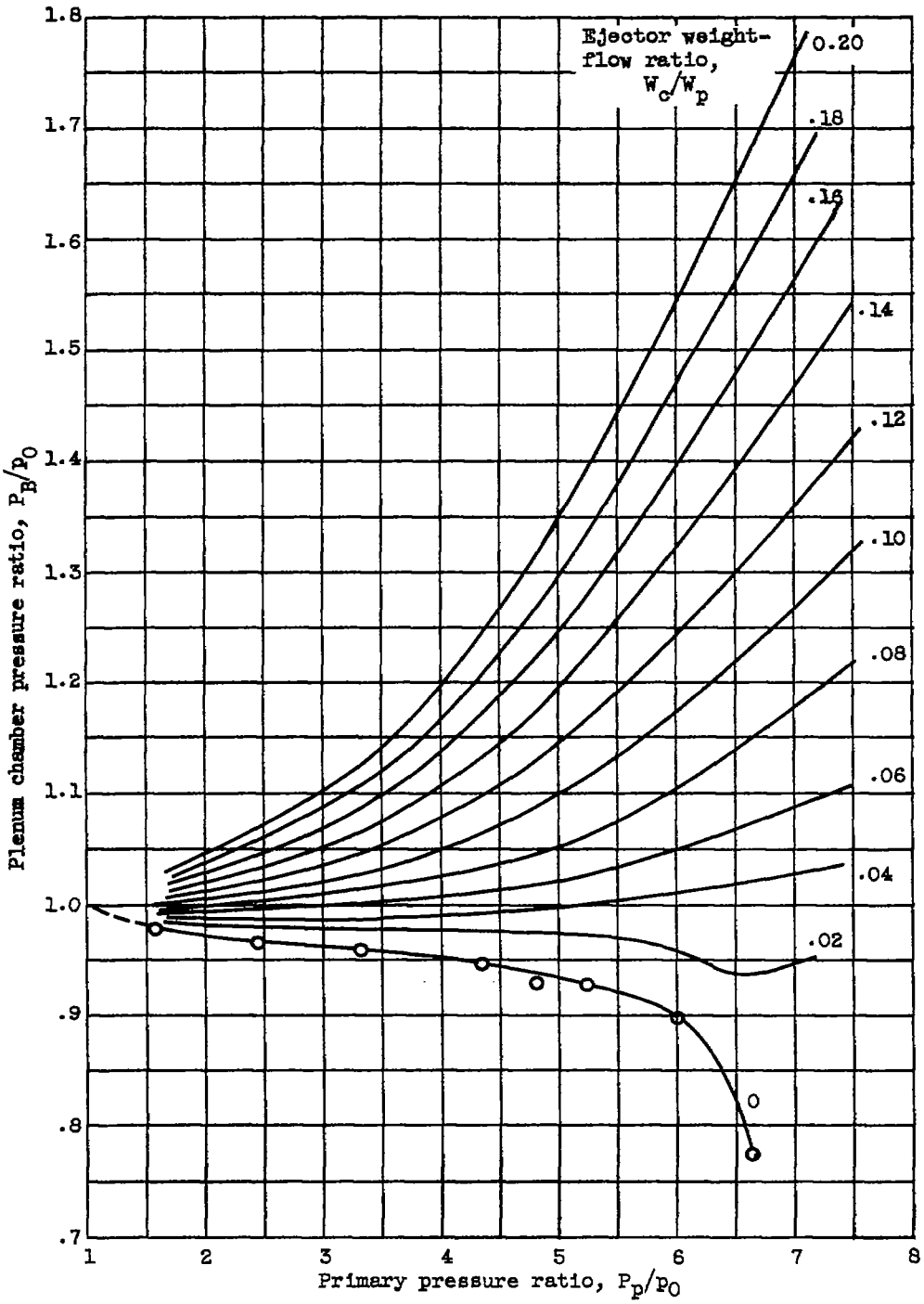

Figure 12. - Pumping characteristics of ejector configuration 3. Primary gas temperatures from 1580° to 1610° R and cooling air supply temperature of 525° R.

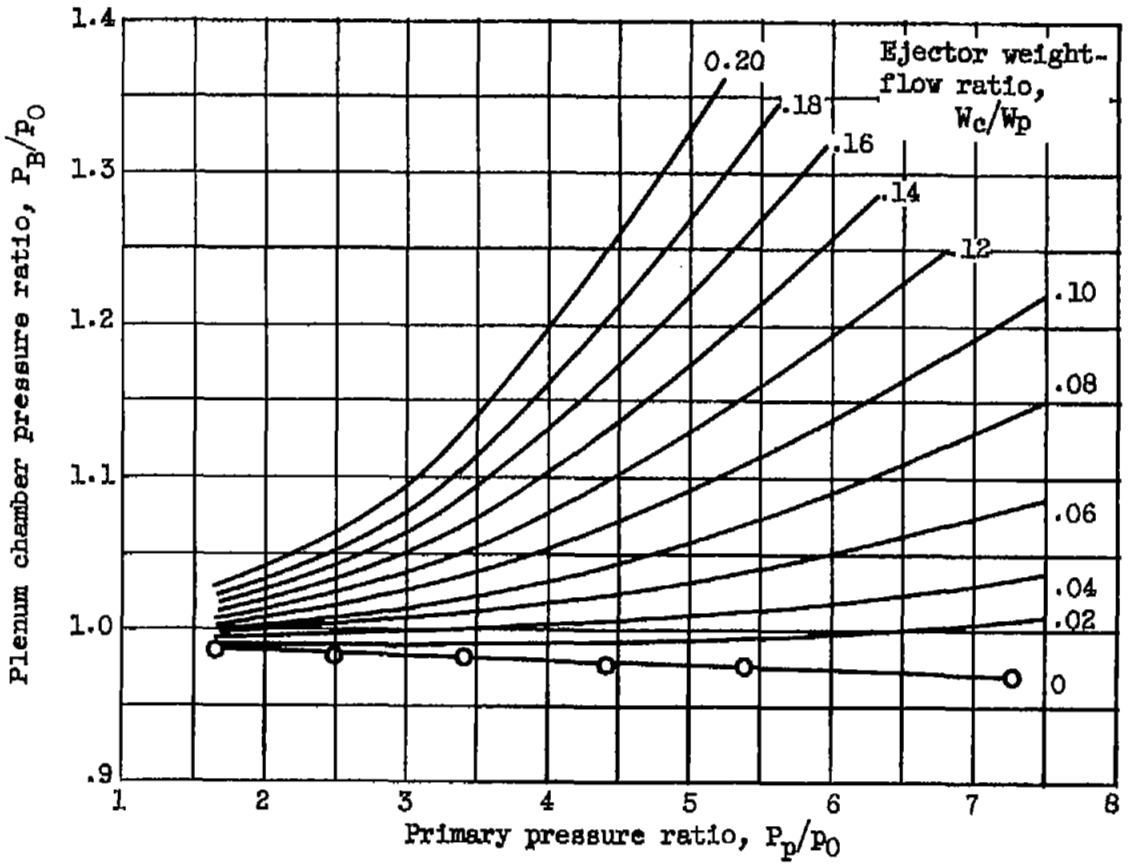

Figure 13. - Pumping characteristics of ejector configuration 4. Primary gas temperatures from 1570° to 1600° R and cooling air supply temperature of 525° R.

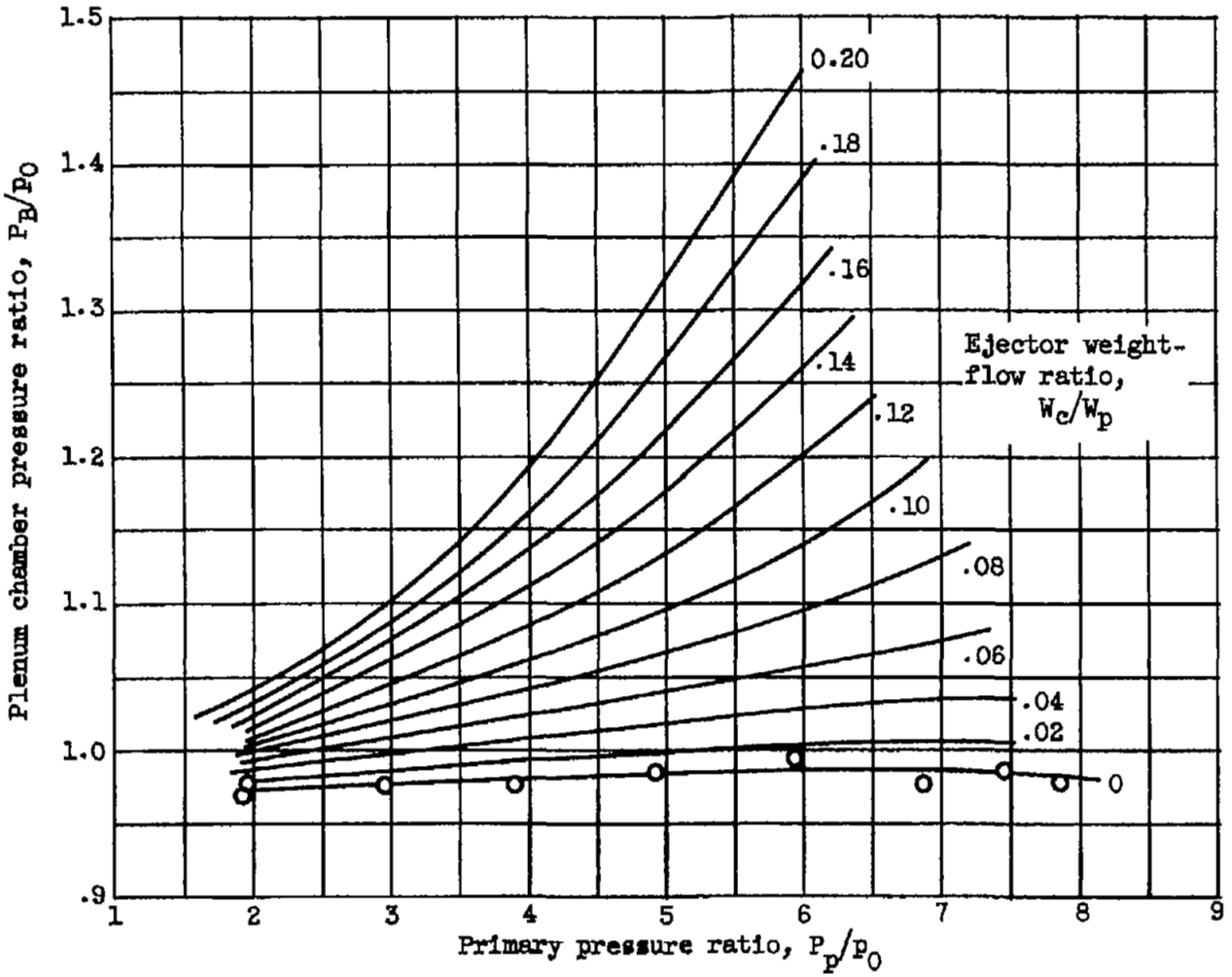

Figure 14. - Pumping characteristics of ejector configuration 5. Primary gas temperatures from 1540° to 1580° R and cooling air supply temperature of 525° R.

3400

CM-4 back

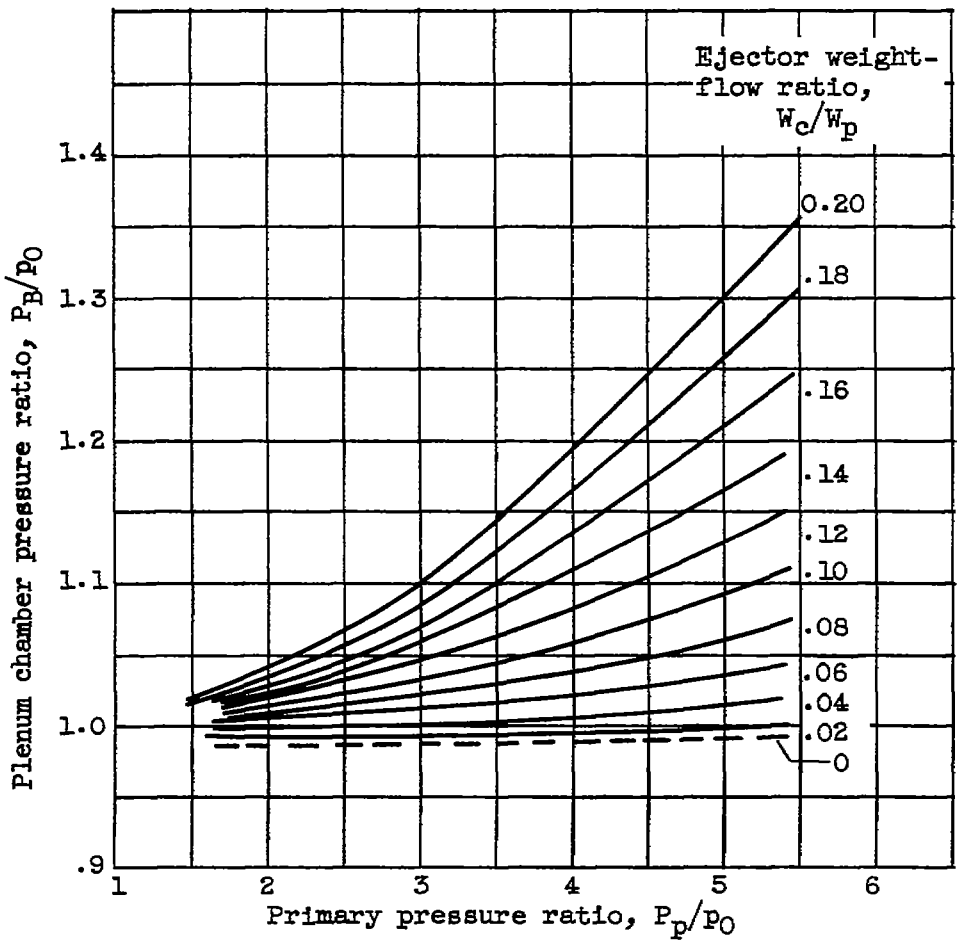

Figure 15. - Pumping characteristics of ejector configuration 6. Primary gas temperatures from 1550° to 1600° R and cooling air supply temperature of 525° R.

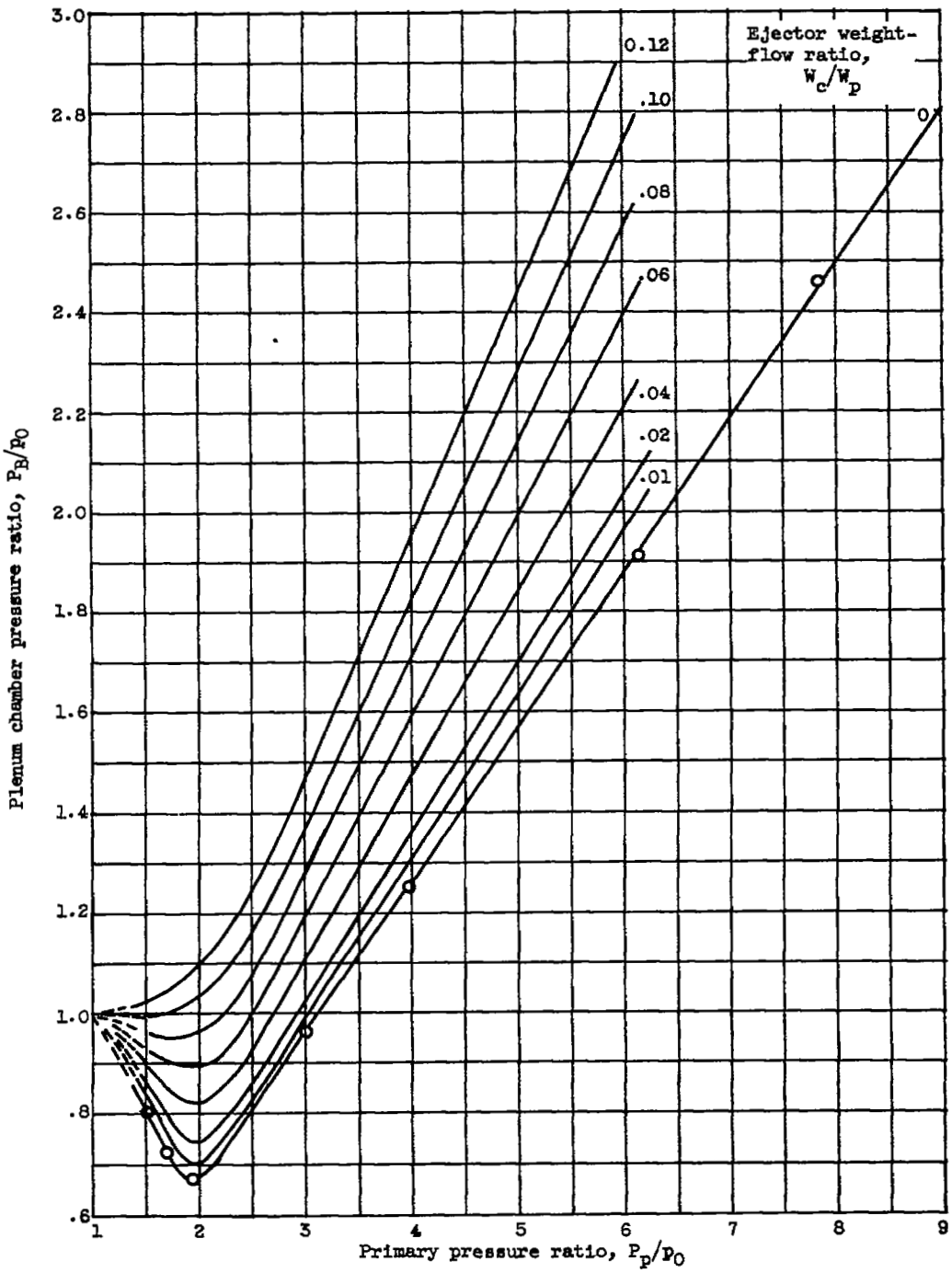

(a) Primary gas temperatures from 2050° to 2200° R.

Figure 16. - Pumping characteristics of ejector configuration 1AB. Cooling air supply temperature of 525° R.

3400

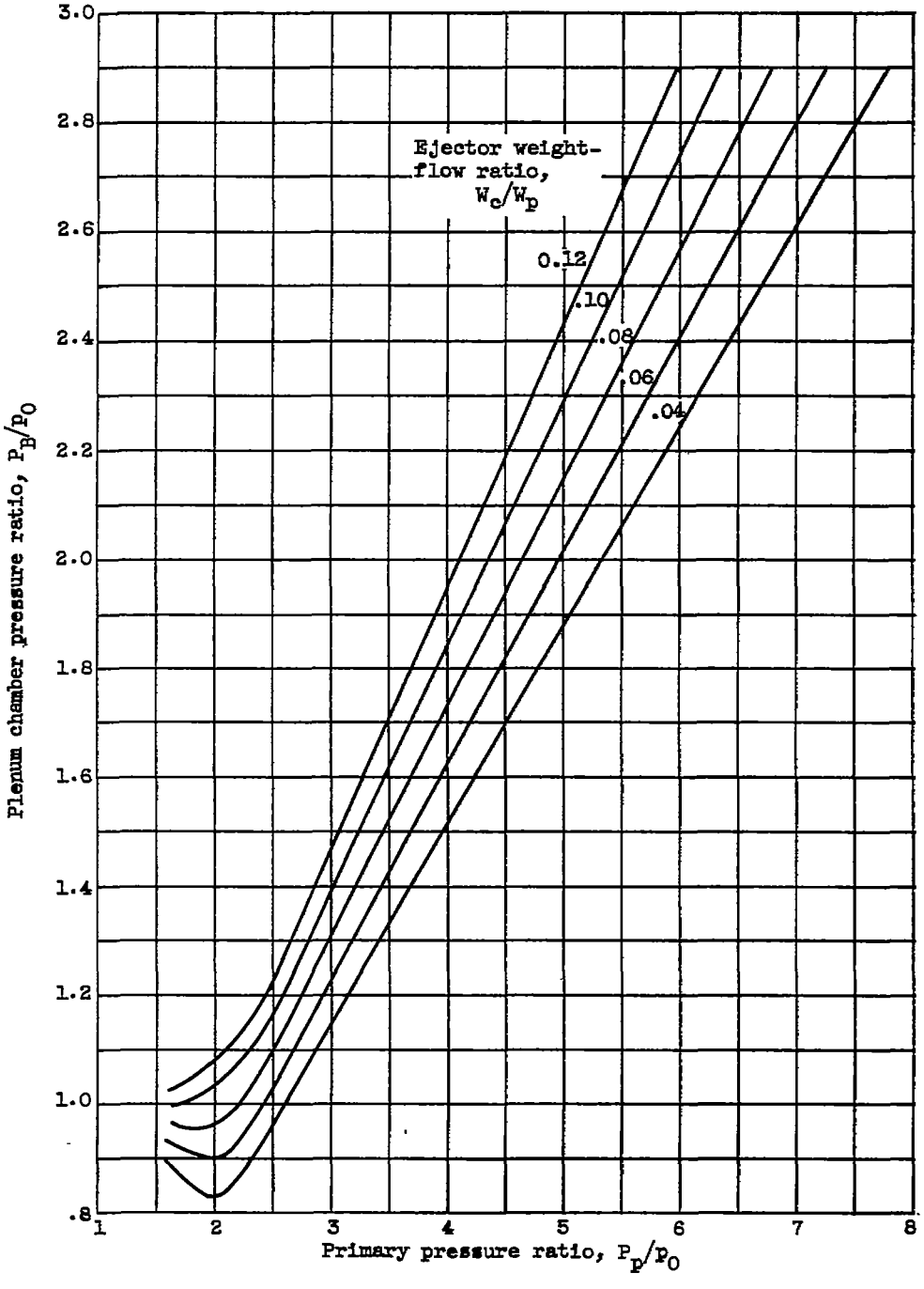

(b) Primary gas temperatures from 2700° to 2800° R.

Figure 16. - Concluded. Pumping characteristics of ejector configuration 1AB. Cooling air supply temperature of 525° R.

3400

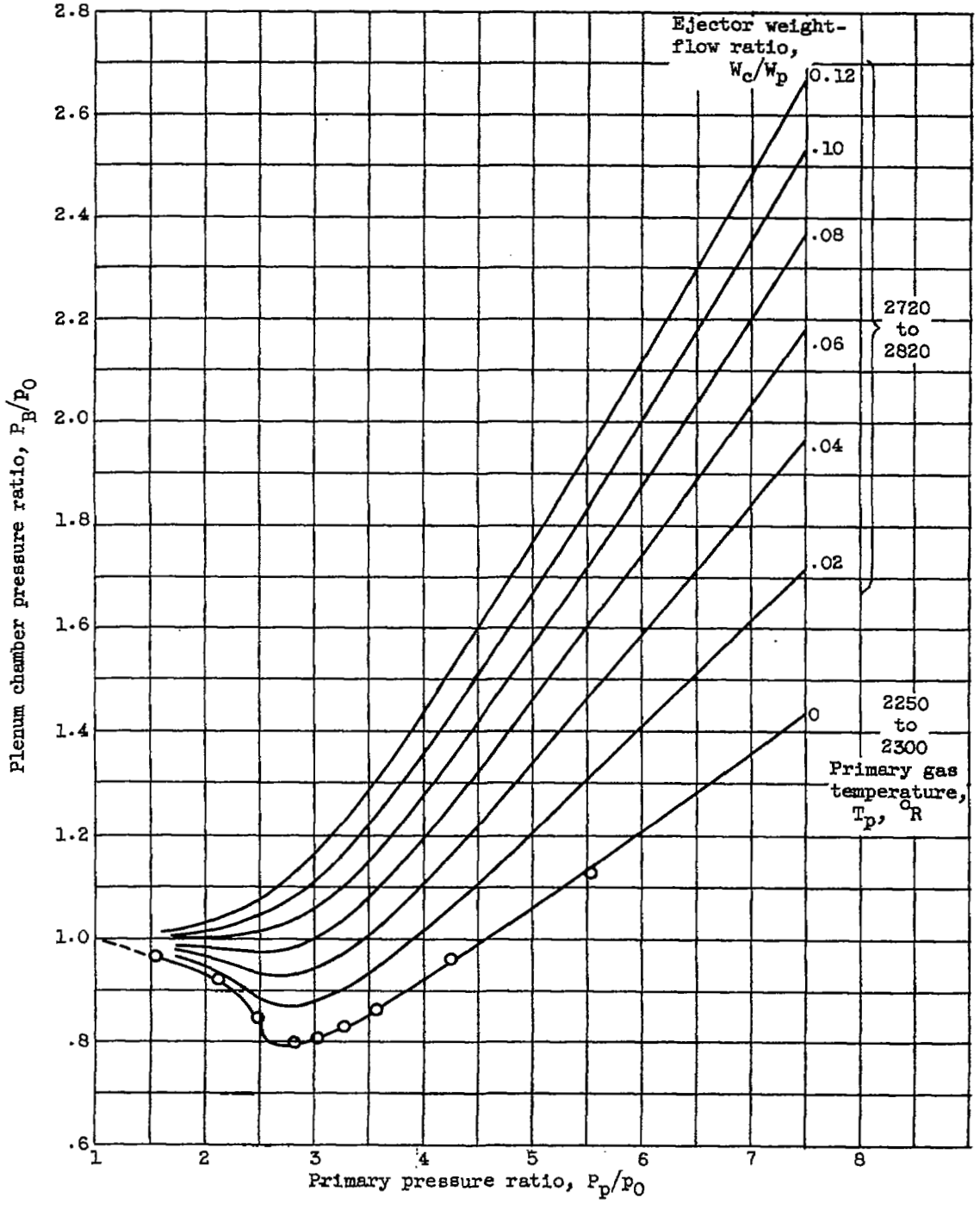

Figure 17. - Pumping characteristics of ejector configuration 3AB. Primary gas temperatures from 2250° to 2820° R and cooling air supply temperature of 525° R.

3400

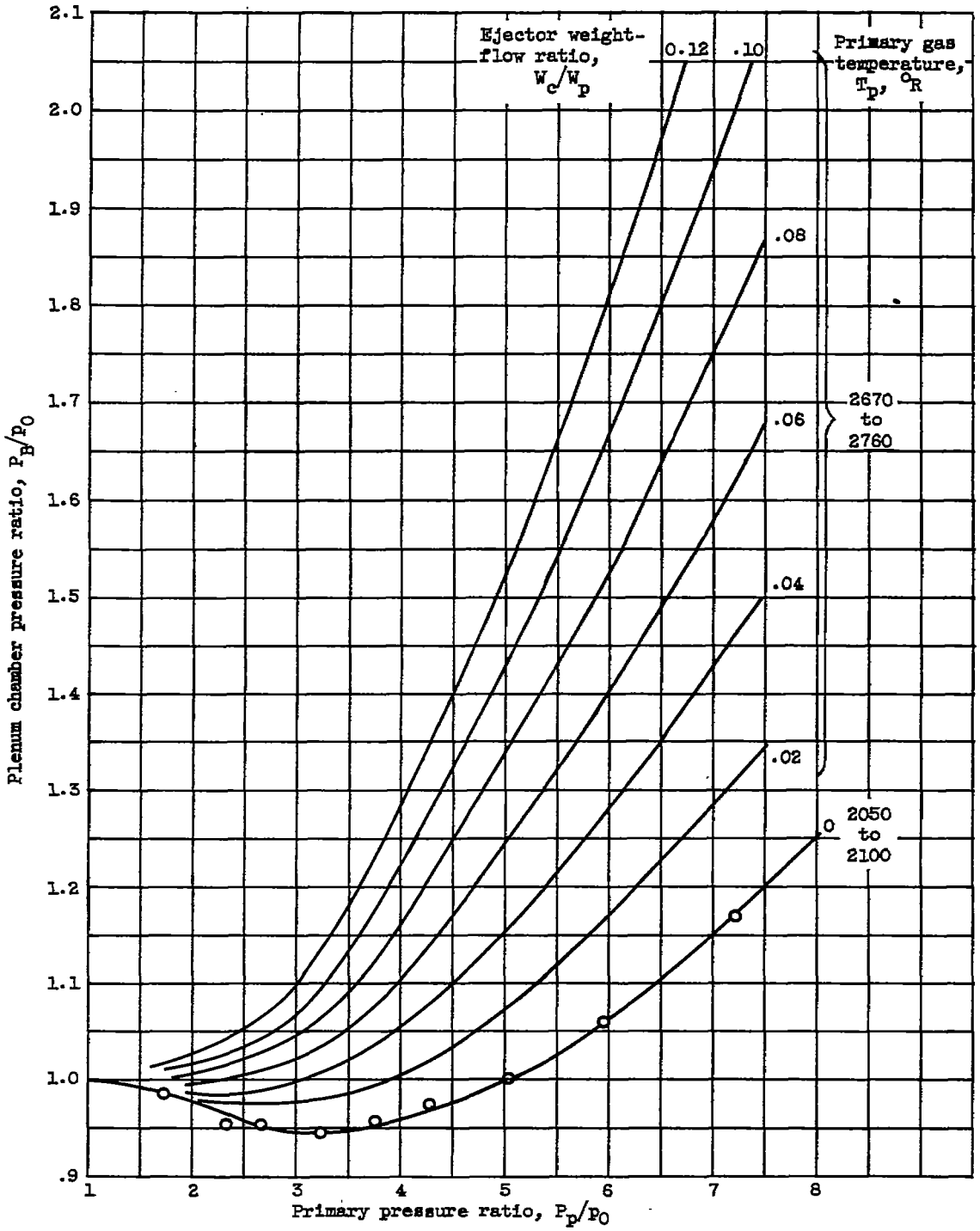

Figure 18. - Pumping characteristics of ejector configuration 4AB. Primary gas temperatures from 2050° to 2760° R and cooling air supply temperature of 525° R.

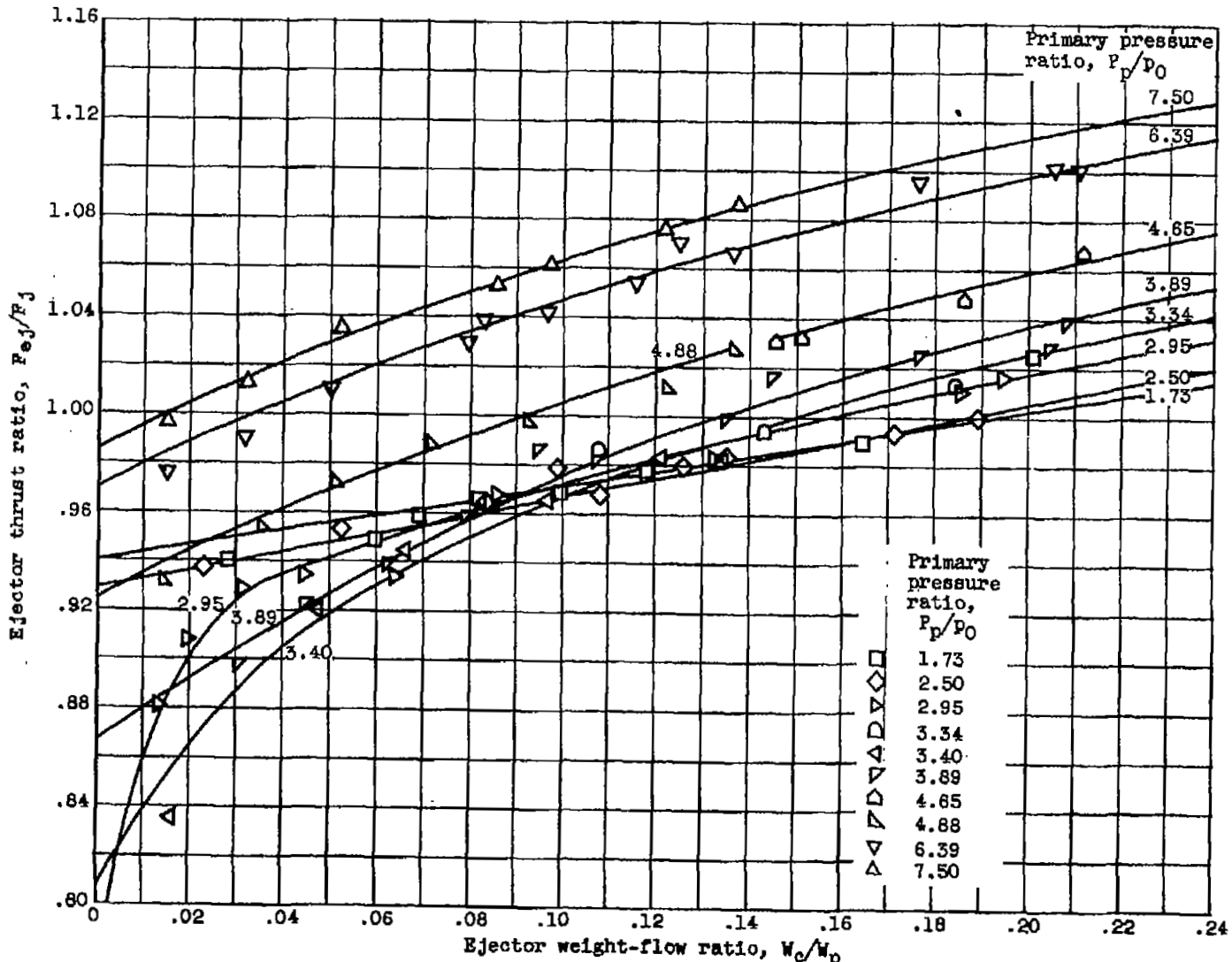

Figure 19. - Thrust data plot of ejector configuration 1. Primary gas temperatures from 1550° to 1580° R and cooling-air supply temperature of 525° R.

[redacted]

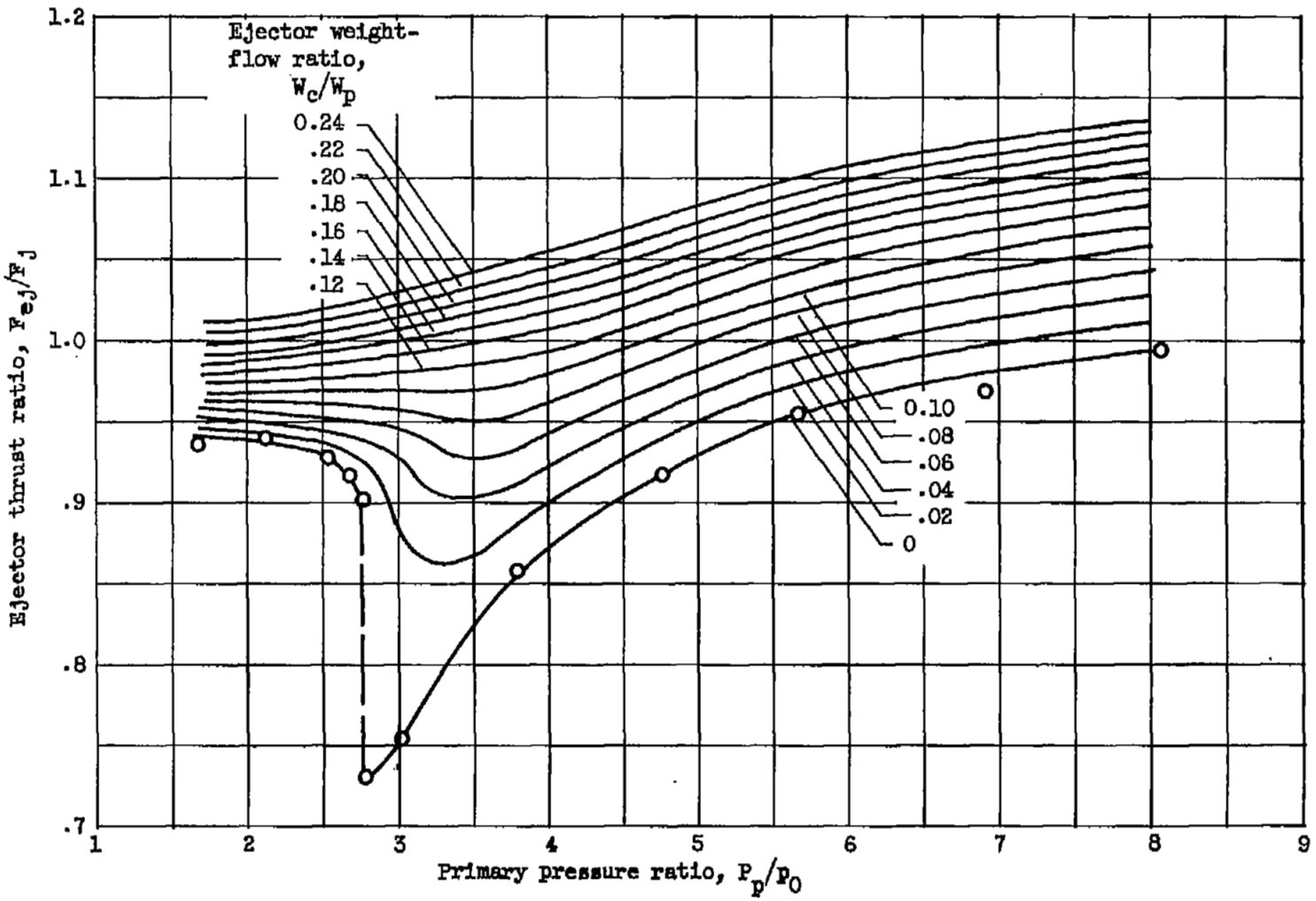

Figure 20. - Thrust characteristics of ejector configuration 1. Primary gas temperatures from 1550° to 1580° R and cooling air supply temperature of 525° R.

[redacted]

3400

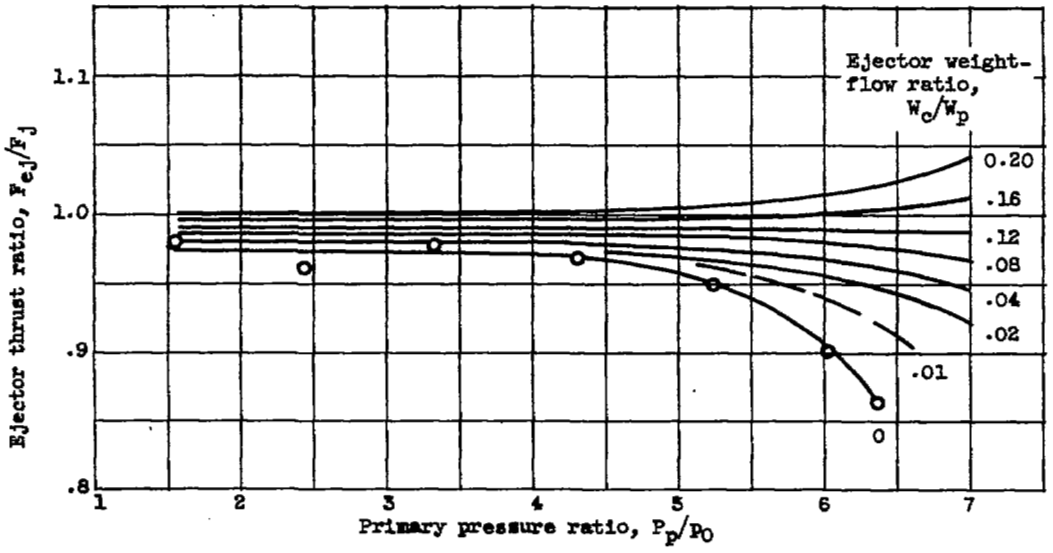

Figure 21. - Thrust characteristics of ejector configuration 3. Primary gas temperatures from 1580° to 1610° R and cooling air supply temperature of 525° R.

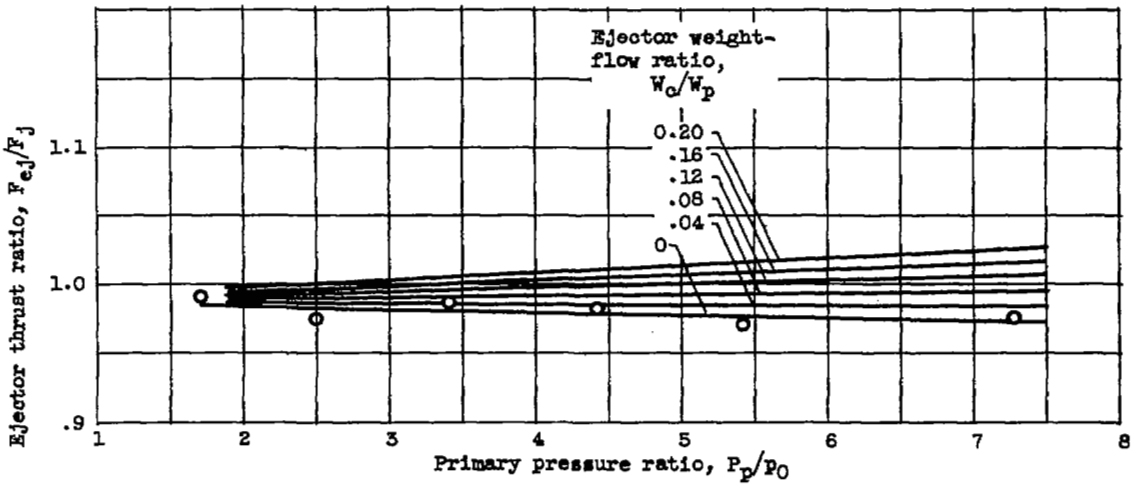

Figure 22. - Thrust characteristics of ejector configuration 4. Primary gas temperatures from 1570° to 1600° R and cooling air supply temperature of 525° R.

CM-5 back 3400

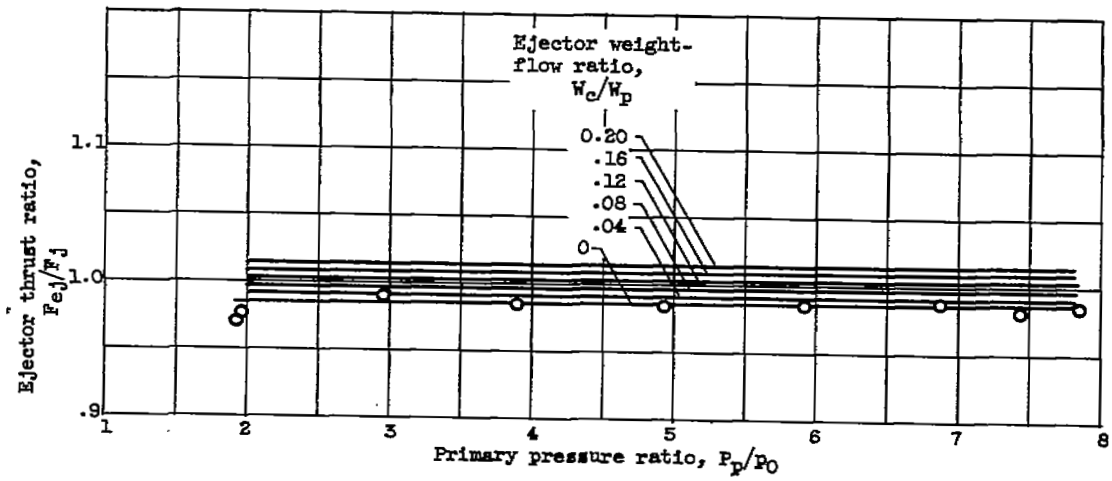

Figure 23. - Thrust characteristics of ejector configuration 5. Primary gas temperatures from 1540° to 1580° R and cooling air supply temperature of 525° R.

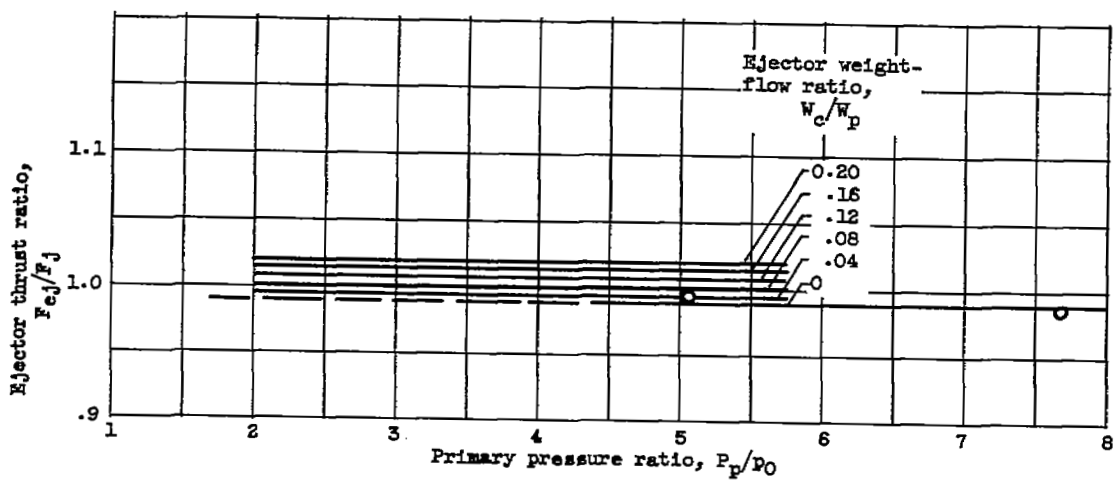

Figure 24. - Thrust characteristics of ejector configuration 6. Primary gas temperatures from 1550° to 1600° R and cooling air supply temperature of 525° R.

3400

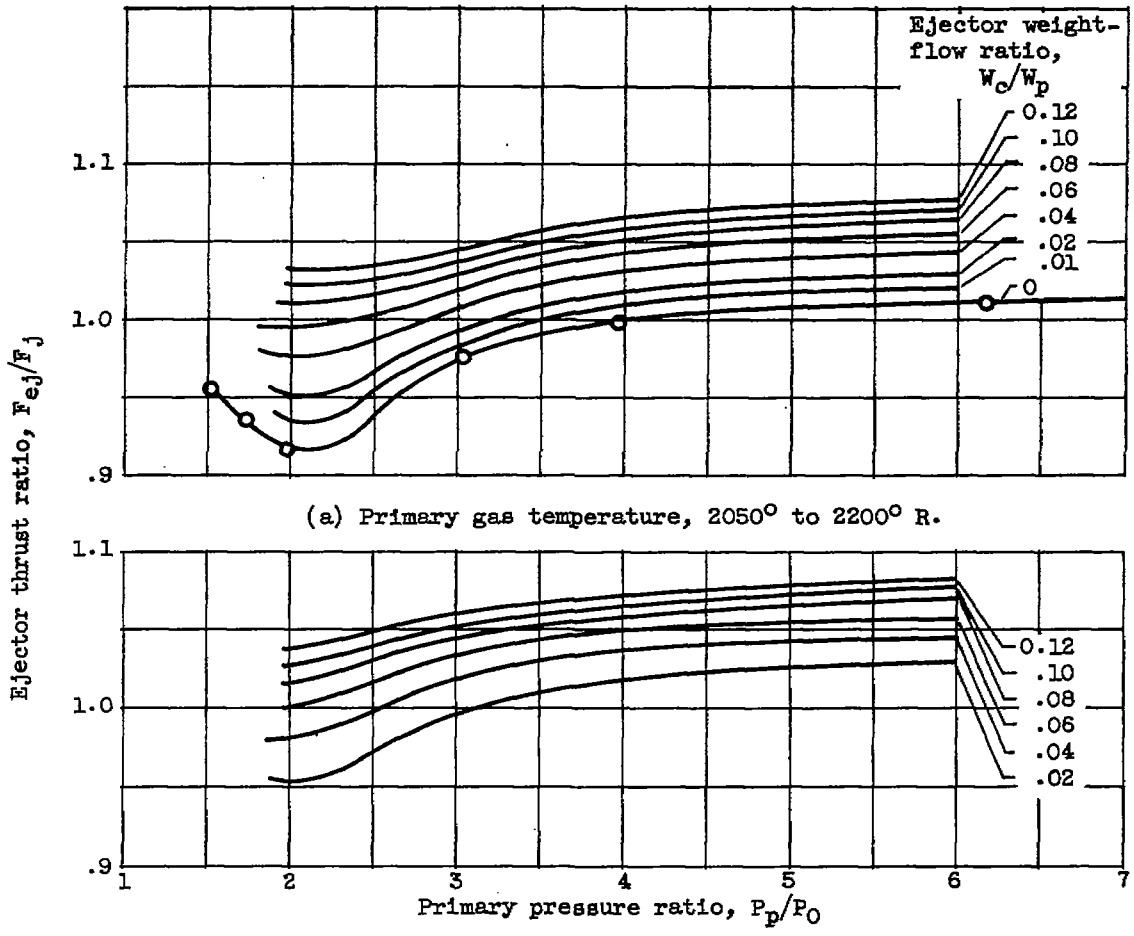

(a) Primary gas temperature, 2050° to 2200° R.

(b) Primary gas temperature, 2700° to 2800° R.

Figure 25. - Thrust characteristics of ejector configuration 1AB. Primary gas temperatures from 2050° to 2800° R and cooling air supply temperature of 525° R.

3400

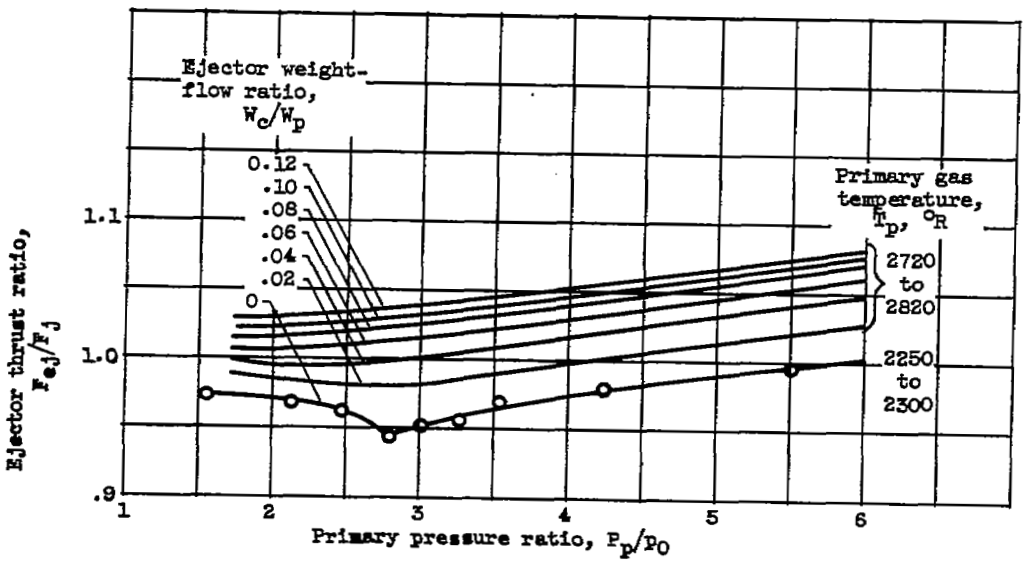

Figure 26. - Thrust characteristics of ejector configuration 3AB. Primary gas temperatures from 2250° to 2820° R and cooling air supply temperature of 525° R.

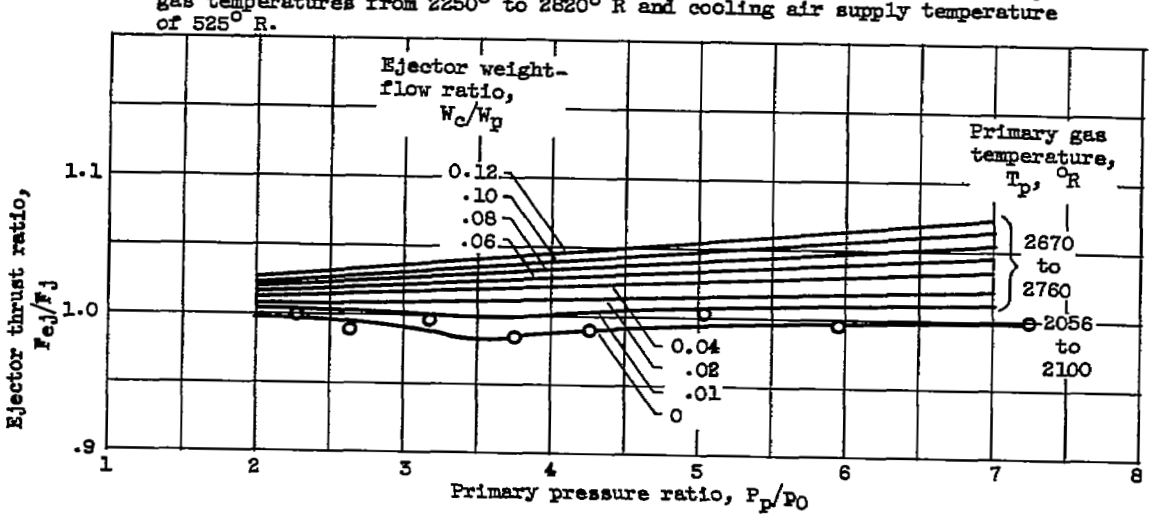

Figure 27. - Thrust characteristics of ejector configuration 4AB. Primary gas temperatures from 2050° to 2760° R and cooling air supply temperature of 525° R.

3400

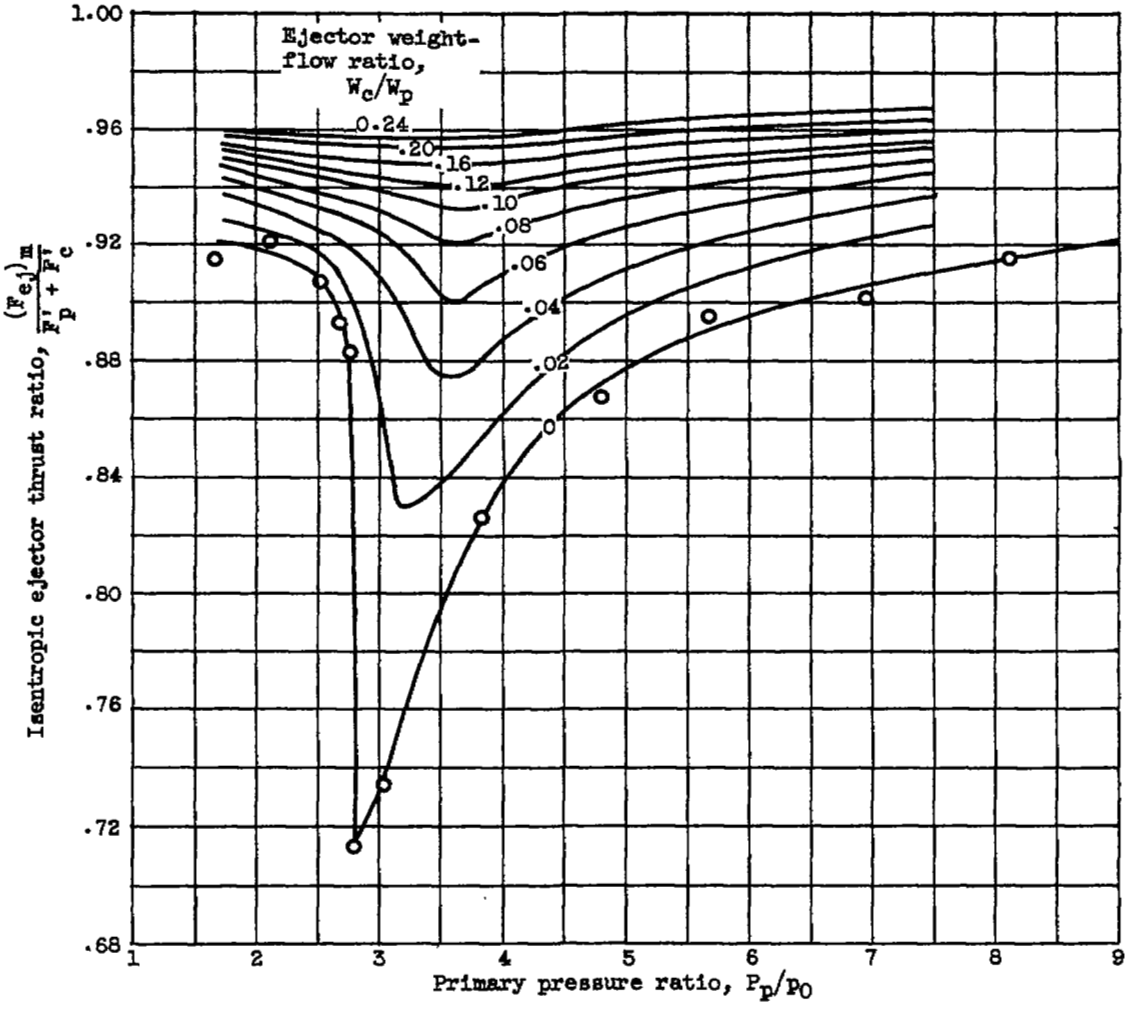

Figure 28. - Isentropic ejector-thrust ratio for ejector configuration 1. Primary gas temperature from 1550° to 1580° R and cooling air supply temperature of 525° R.

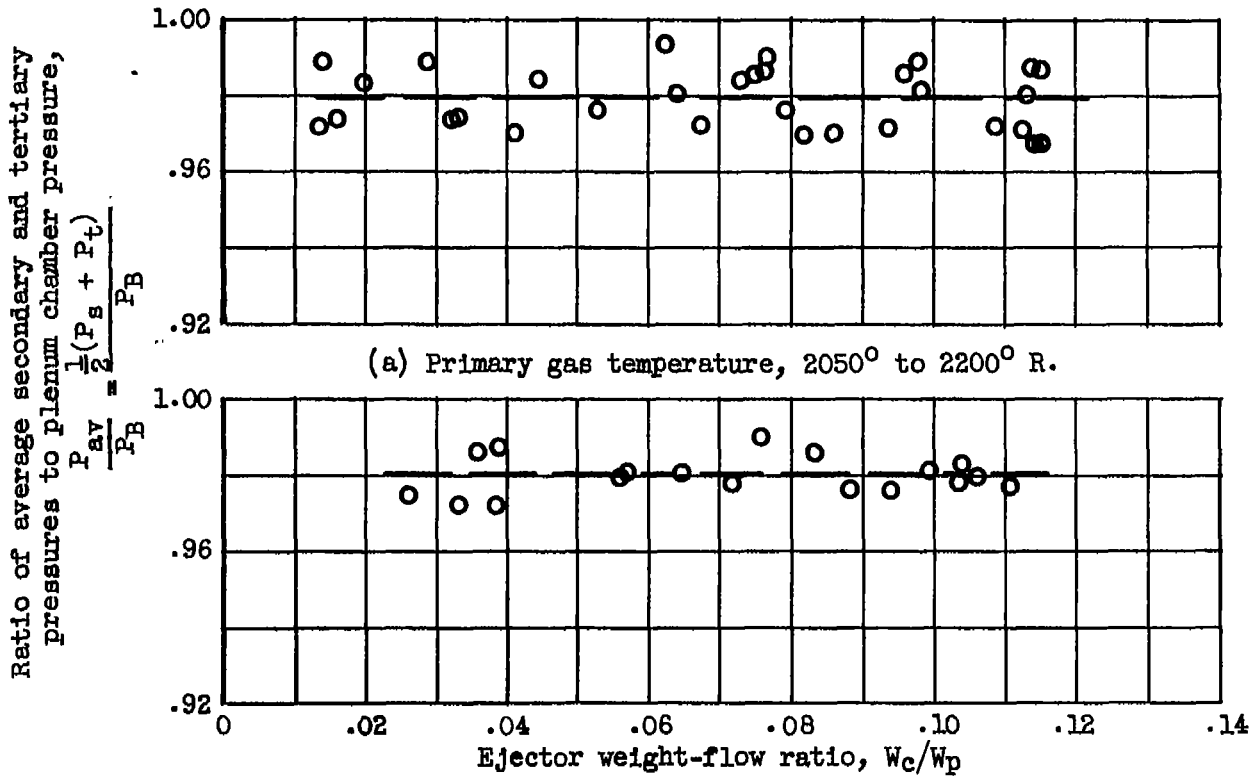

(a) Primary gas temperature, 2050° to 2200° R.

(b) Primary gas temperature, 2700° to 2800° R.

Figure 29. - Ratio of average total pressure in secondary and tertiary passages to plenum chamber pressure for ejector configuration 1AB. Primary gas temperatures from 2050° to 2800° R and cooling air supply temperature of 525° R.

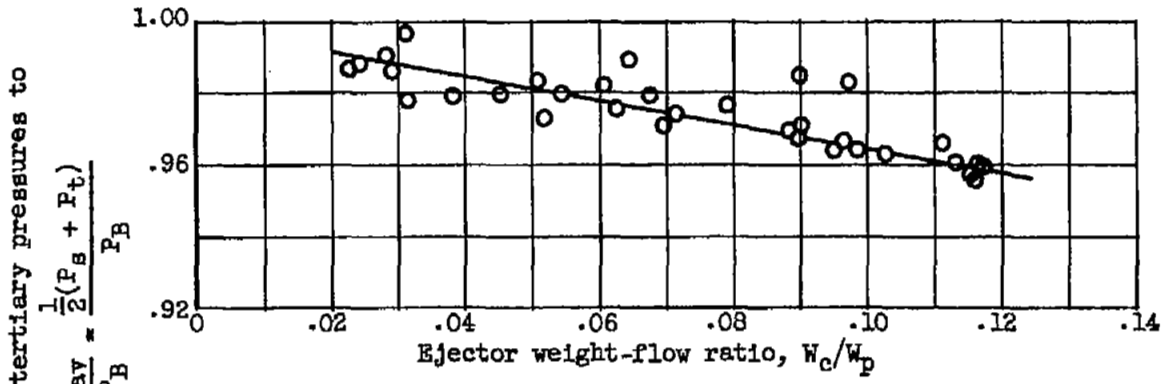

Figure 30. - Ratio of average total pressure in secondary and tertiary passages to plenum chamber pressure for ejector configuration 3AB. Primary gas temperatures from 2720° to 2820° R and cooling air supply temperature of 525° R.

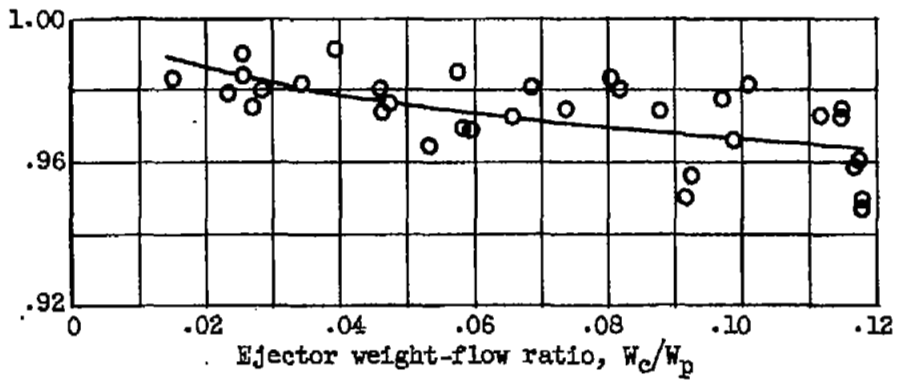

Figure 31. - Ratio of average total pressure in secondary and tertiary passages to plenum chamber pressure for ejector configuration 4AB. Primary gas temperatures from 2670° to 2760° R and cooling air supply temperature of 525° R.

3400

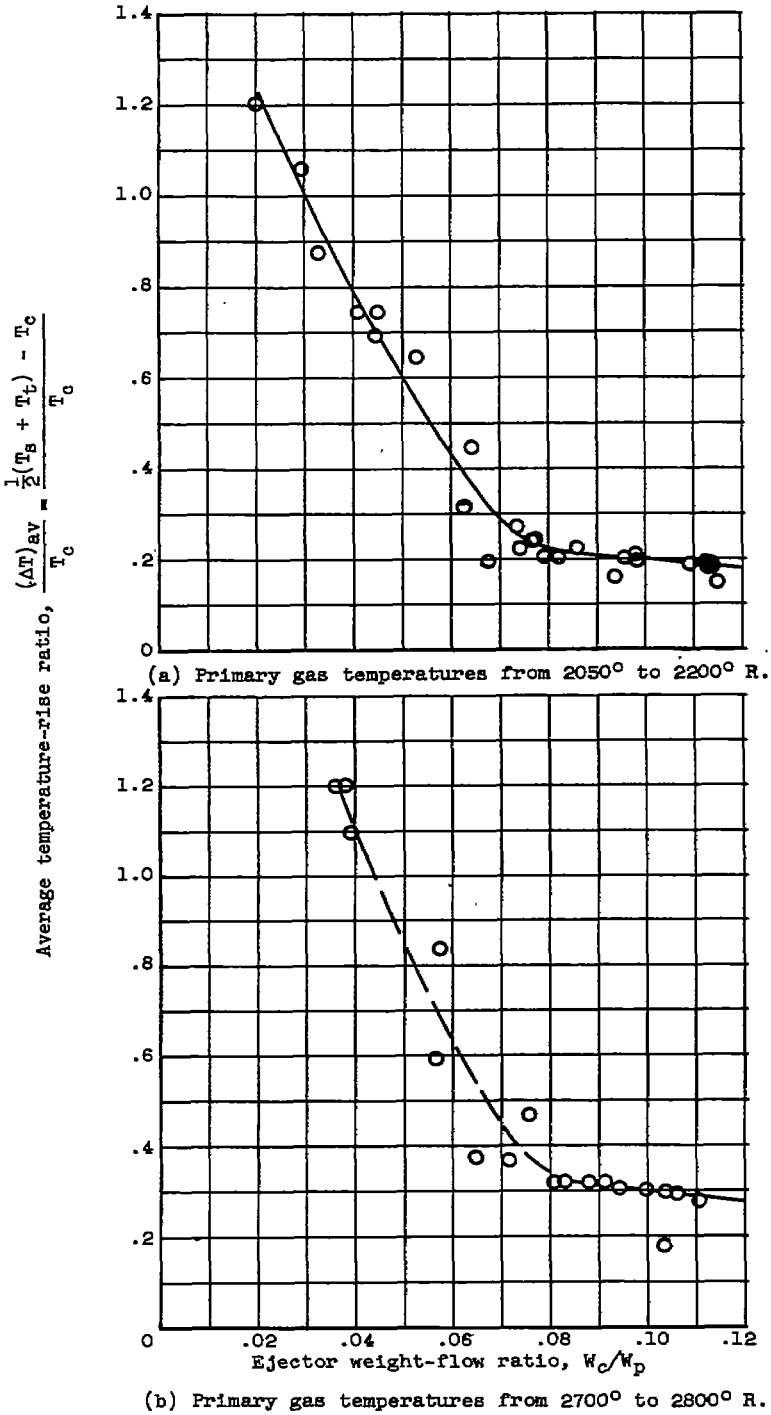

(a) Primary gas temperatures from 2050° to 2200° R.

(b) Primary gas temperatures from 2700° to 2800° R.

Figure 32. - Average temperature-rise ratio for ejector configuration 1AB. Cooling air supply temperature of 525° R.

[redacted]

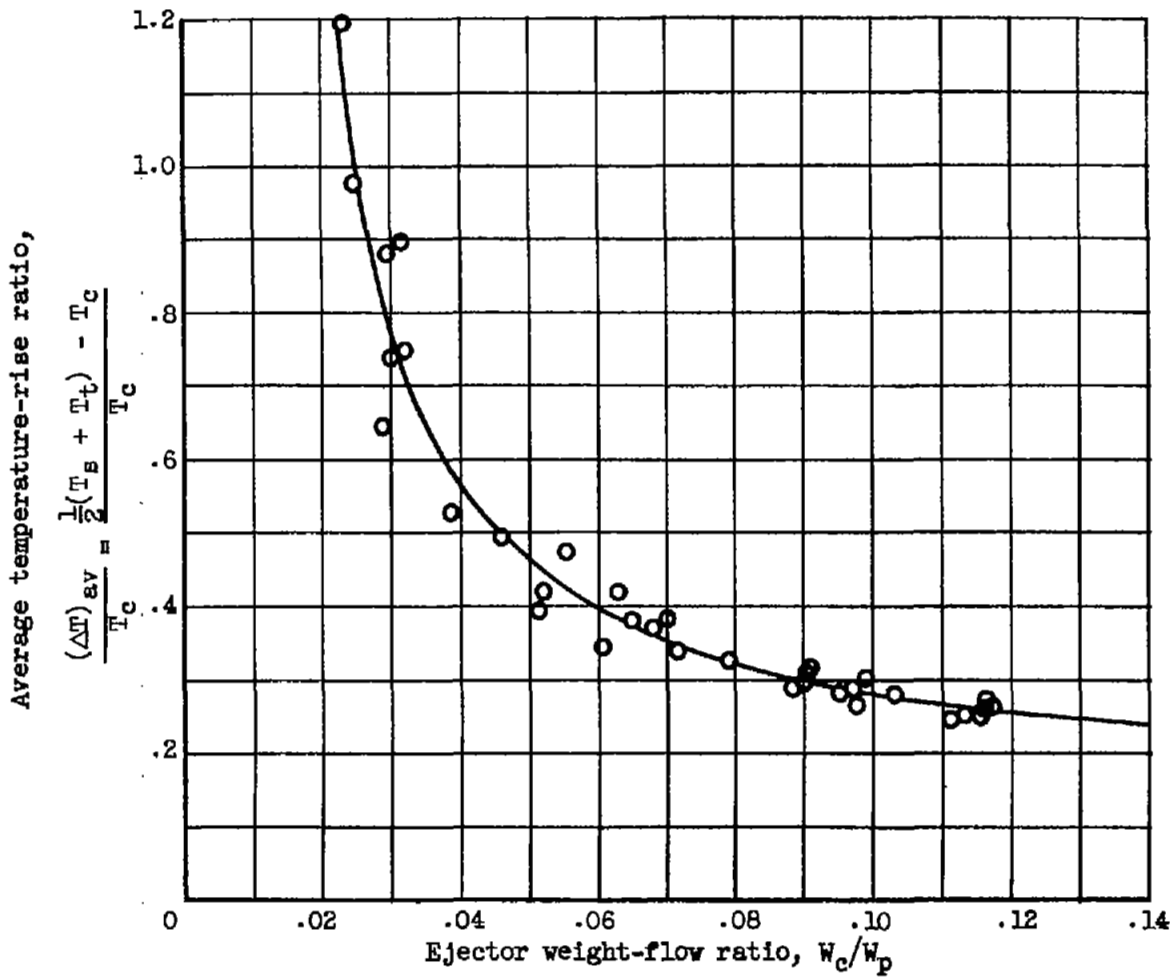

Figure 33. - Average temperature-rise ratio for ejector configuration 3AB. Primary gas temperatures from 2720° to 2820° R and cooling air supply temperature of 525° R.

[redacted]

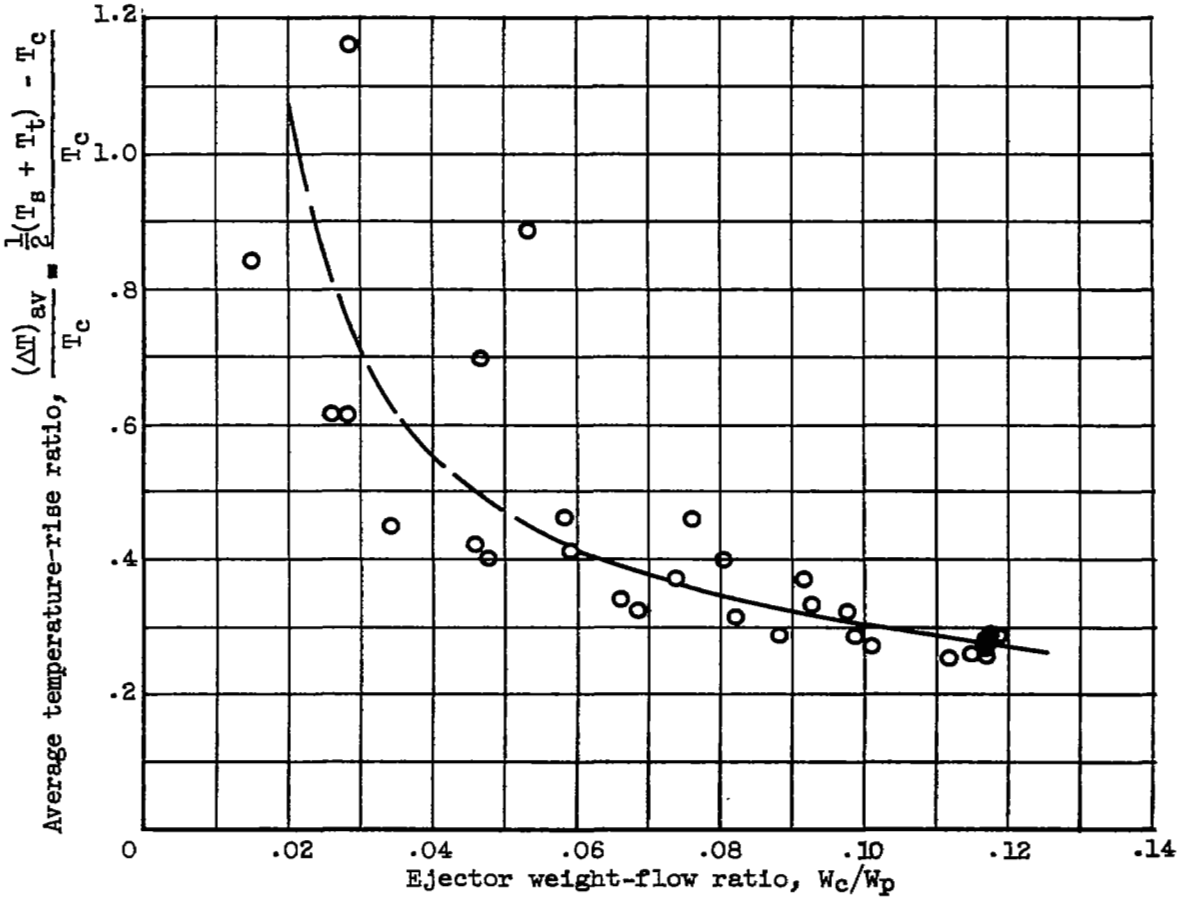

Figure 34. - Average temperature-rise ratio for ejector configuration 4AB. Primary gas temperatures from 2670° to 2760° R and cooling air supply temperature of 525° R.

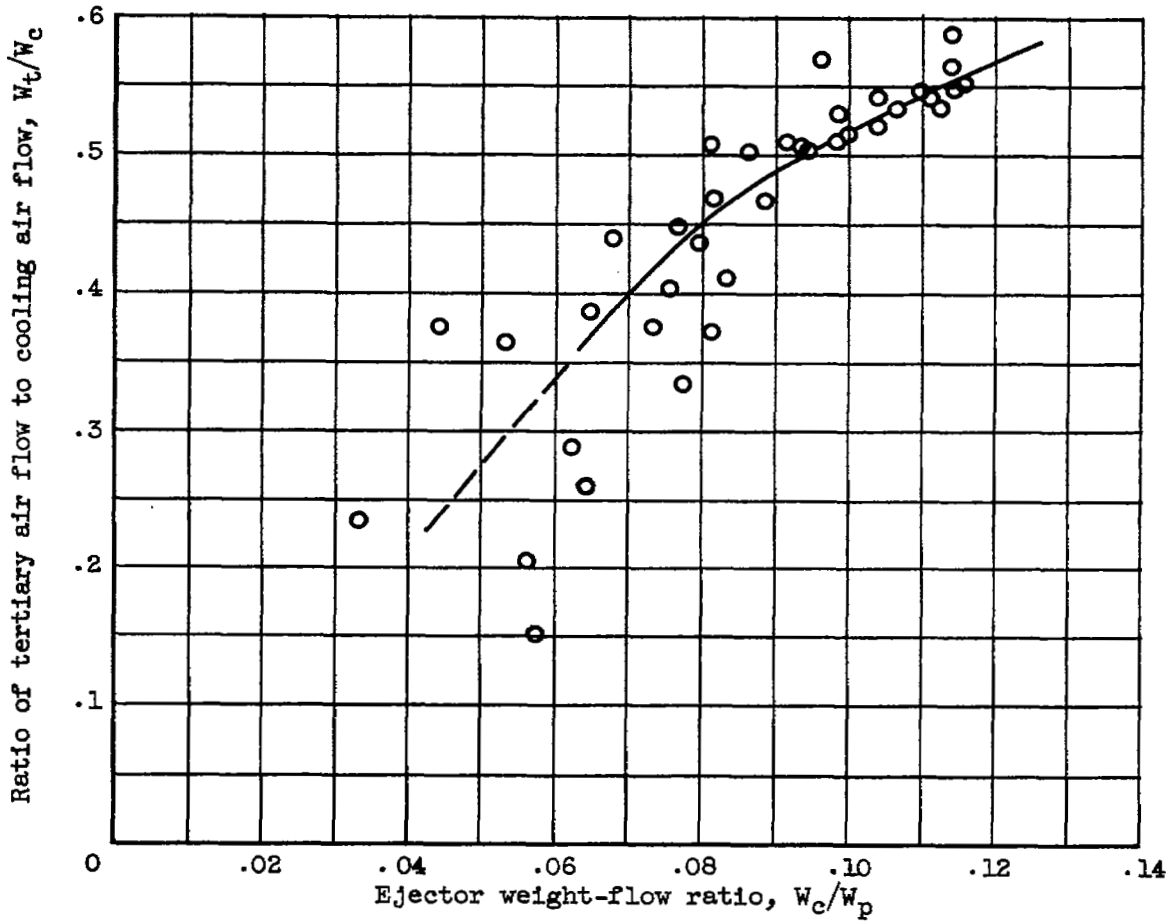

Figure 35. - Ratio of tertiary to total cooling air flow for ejector configuration 1AB. Primary gas temperatures from 2050° to 2800° R and cooling air supply temperature of 525° R. $W_s/W_c = 1 - W_t/W_c$.

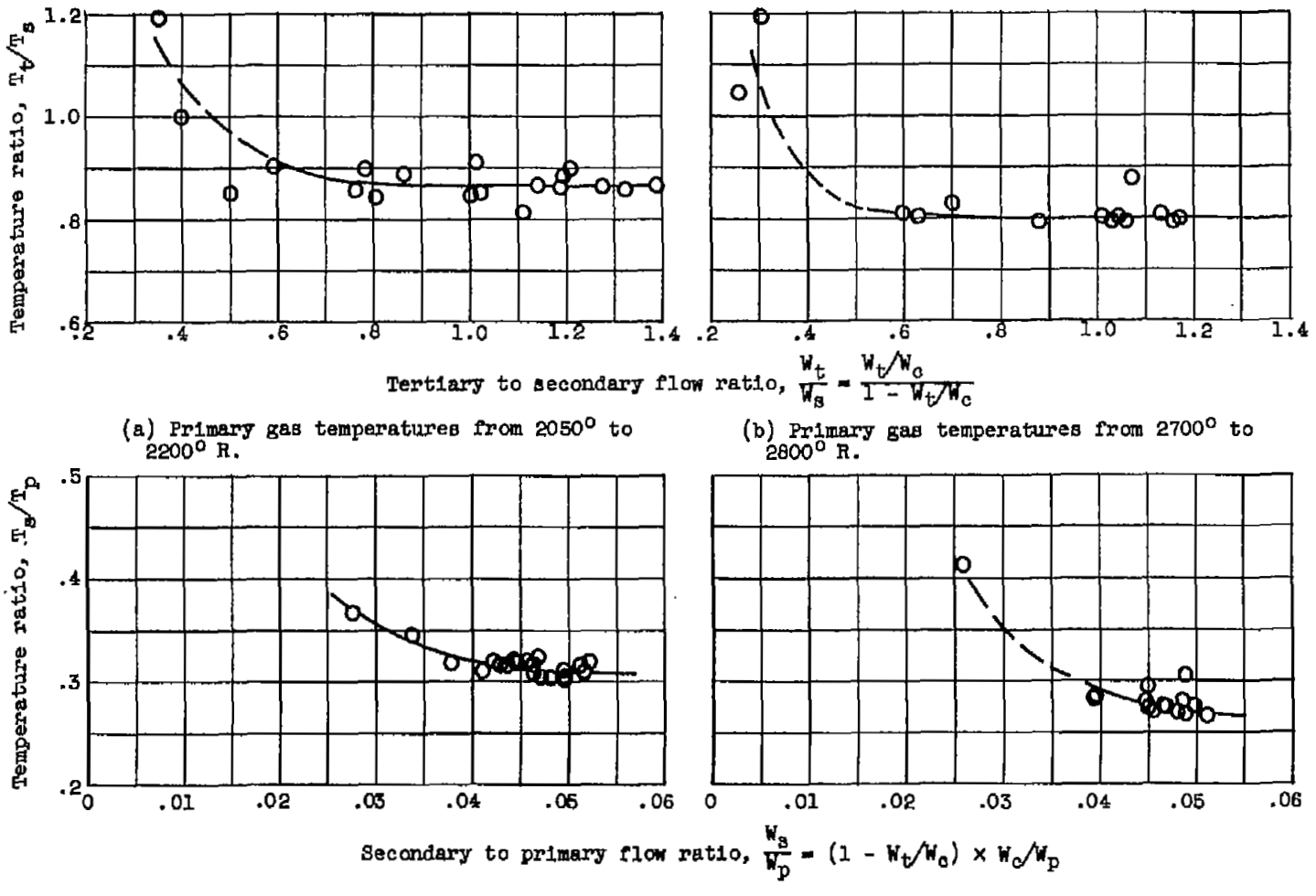

(a) Primary gas temperatures from 2050° to 2200° R.

(b) Primary gas temperatures from 2700° to 2800° R.

(c) Primary gas temperatures from 2050° to 2200° R.

(d) Primary gas temperatures from 2700° to to 2800° R.

Figure 36. - Temperature ratio against flow ratio for secondary and tertiary passages of ejector configuration 1AB at two primary gas temperatures. Cooling air supply temperature of 525° R.

NACA-Langley - 8-19-54 - 350

NASA Technical Library
3 1176 01435 4139